Interactions of ATP with the Dynein-tubulin System of Cilia from Tetrahymena pyriformis

Masami TAKAHASHI

CONTENTS

ABBREVIATIONS

Chemicals

DTT	Dithiothreitol
EGTA	Ethyleneglycol-bis(β-aminoethylether)-N,N,N,',N'-tetraacetate
PEP	Phosphoenol pyruvate
SDS	Sodium dodecyl sulfate
TCA	Trichloroacetic acid

Nucleotides

NTP	Nucleoside 5'-triphosphate
2'-dATP	2'-Deoxy-ATP
3'-dATP	3'-Deoxy ATP
εATP	$1,N^6$-etheno-ATP
FTP	Formycin 5'-triphosphate
8-NH(CH_3)-ATP	8-Monomethylamino-ATP
8,3'-S-cyclo-ATP	8,3'-Anhydro-8-mercapto-9-β-D-xylofuranosyl-adenine 5'-triphosphate
8-Br-ATP	8-Bromo-ATP
8-SCH_3-ATP	8-Methylmercapto-ATP
8-OCH_3-ATP	8-Methoxy-ATP
AMPPNP	Adenylyl imidodiphosphate

INTRODUCTION

Cell motility is one of the most interesting and important problems of energy transformation in living organisms. Cilia and flagella of eukaryotes are motile hair-like organelles projecting from the free surface of cells. They occur in most groups of animals and plants except crustacea, angiosperms, and gymnosperms. They produce the motile force to cause fluid to move, propelling the cell or moving material along a ciliated tract.

Numerous studies with electron microscopes have established that all cilia and flagella of eukaryotes possess essentially the same fine structure. A brief diagram of cross section of cilia and flagella of eukaryotes is illustrated in Fig. 1 (1). Cilia and flagella are approximately cylindrical, enclosed by a cell membrane, and composed of nine outer doublet microtubules and two central microtubules. The central pair of microtubules are enclosed by a complex protein sheath. The outer doublet microtubules and central tubules are held together at frequent intervals along their length by spokes that extend radially from the A-tubules of the outer doublets to central sheath. The outer doublet tubules are connected to one another by an elastic linkage named nexin. The A-tubule of each outer doublet is a complete-tubule and bears the two rows of arms that extend toward the B-tubule of the adjacent doublet. The B-tubule is an incomplete C-shaped tubule and shares a part of the wall of the A-tubule. All these microtubules are known to be composed of globular protein named tubulin, which is different from actin, one of the contractile protein of muscle, in several respects as summarized in Table

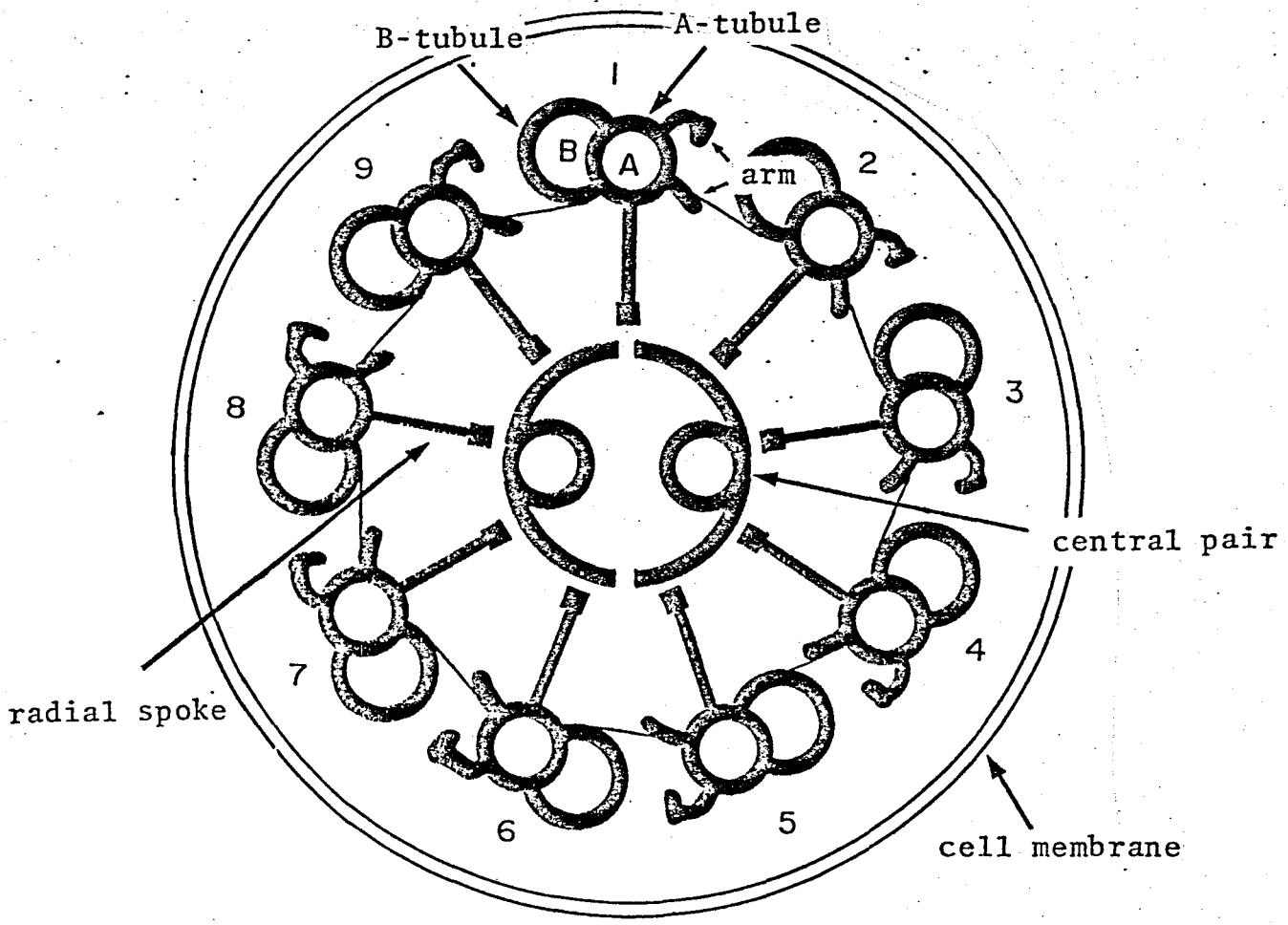

Fig. 1. Diagram of cross section of cilia and flagella of eukaryotes.

Table I. Comparison of Tubulin and Actin

	Tubulin	Actin
Polymer	Microtubule	Filament
Physiological unit	Heterodimer($\alpha\beta$)	Monomer(G-actin)
Molecular weight of subunit	50,000-58,000	42,000
Bound nucleotide	GDP, GTP	ADP, ATP
Colchicine binding	+	-
Interaction with myosin		
superprecipitation	+	+
activation of Mg^{2+}-ATPase	+	+
Amino acid composition	different from each other	
Antigenecity	different from each other	

I (2).

Since the discovery of ATPase [EC 3.6.1.3] activity in sperm flagella (3,4) and the demonstration that glycerinated sperm can be reactivated with ATP (5), it has been generally accepted that the energy for motility in cilia and flagella is provided by dephosphorylation of ATP.

Gibbons (6,7) showed that most of the ATPase is localized in the arm by selective extraction and recombination of the axonemes, (demembraned cilia or flagella), combined with electron microscopy. He named the ATPase dynein. Later, Ogawa et al. (8) also immunologically showed that dynein is localized in the outer arm of axonemes.

Dynein was purified from Tetrahymena cilia by Gibbons (9) and from sea urchin sperm flagella by Mohri et al.(10) and by others (11,12). The properties of dynein are much different from that of myosin, an ATPase of muscle, as summarized in Table II(2).

As for the role of dynein in the ciliary and the flagellar movement, it was shown that the nucleotide specificity and the cation requirement in the motility of reactivated cilia and flagella closely resembled those in dynein ATPase (9,18,19). Furthermore, Gibbons and Gibbons (20) showed that when dynein arms were extracted from sea urchin sperm flagella, the decrease in the number of dynein arms on the doublets accurately parallels the decrease in the beat frequency of the flagella. Gibbons and Gibbons (21) showed that the mobility was recovered when the dynein rebound to the outer doublet defficient of arms. In addition, Okuno et al. (22) and Gibbons et al.(23) showed that antiserum against the subfragment of dynein inhibited the motility of reactivated flagella.

Table II. Comparison of Dynein and Myosin

	Dynein	Myosin
Molecular shape	Globular	Rod
Molecular weight of subunit	$3.5\text{-}5.5 \times 10^5$ (13-16)	2.0×10^5
Solubility under the low ionic strength	Soluble	Insoluble
ATPase activity in the presence of Mg^{2+}	High	Low
ATPase activity in the presence of EDTA	Very low	High
Effect of vanadate on ATPase activity	Inhibited (17)	Not inhibited
Substrate specificity	Highly specific for ATP	Not so specific for ATP

From these evidences it is generally accepted that dynein plays a major role in generating the bending movement of cilia and flagella.

In 1968, Satir (24) showed by electron microscopy that the overall length of ciliary microtubules remained constant during bending, proposing that the bending was induced not by a contraction but by a sliding between microtubules. Summers and Gibbons (25) showed by dark-field light microscopy that addition of ATP to axonemes, which had been briefly predigested with trypsin, caused active sliding movements between the doublet tubules of the axonemes. These findings indicate that the bending movement of cilia and flagella of eukaryotes results from an active sliding movement between adjacent doublet tubules of the axoneme (cf. Fig. 2). Sale and Satir (26) showed that each doublet actively slides relative to its neighbors in a single direction, and the polarity of force generation of the dynein arm in sliding is from the base to the tip.

According to Brokaw (27), many properties of cilia and flagellar movement can be explained by adopting the two- or three-state model proposed by A. F. Huxley (28) for muscle contraction. Thus, the mechanochemical cycle in cilia and flagella consists of the following three elementary processes: (1) attachment of the dynein arm located on the A-tubule to an adjacent B-tubule to form a cross-bridge, (2) conformational change or functional movement of the cross-bridge, and (3) detachment of the dynein arm from the B-tubule.

However, no clear evidence for the conformational change in the dynein arm has been reported. Furthermore, two conflict-

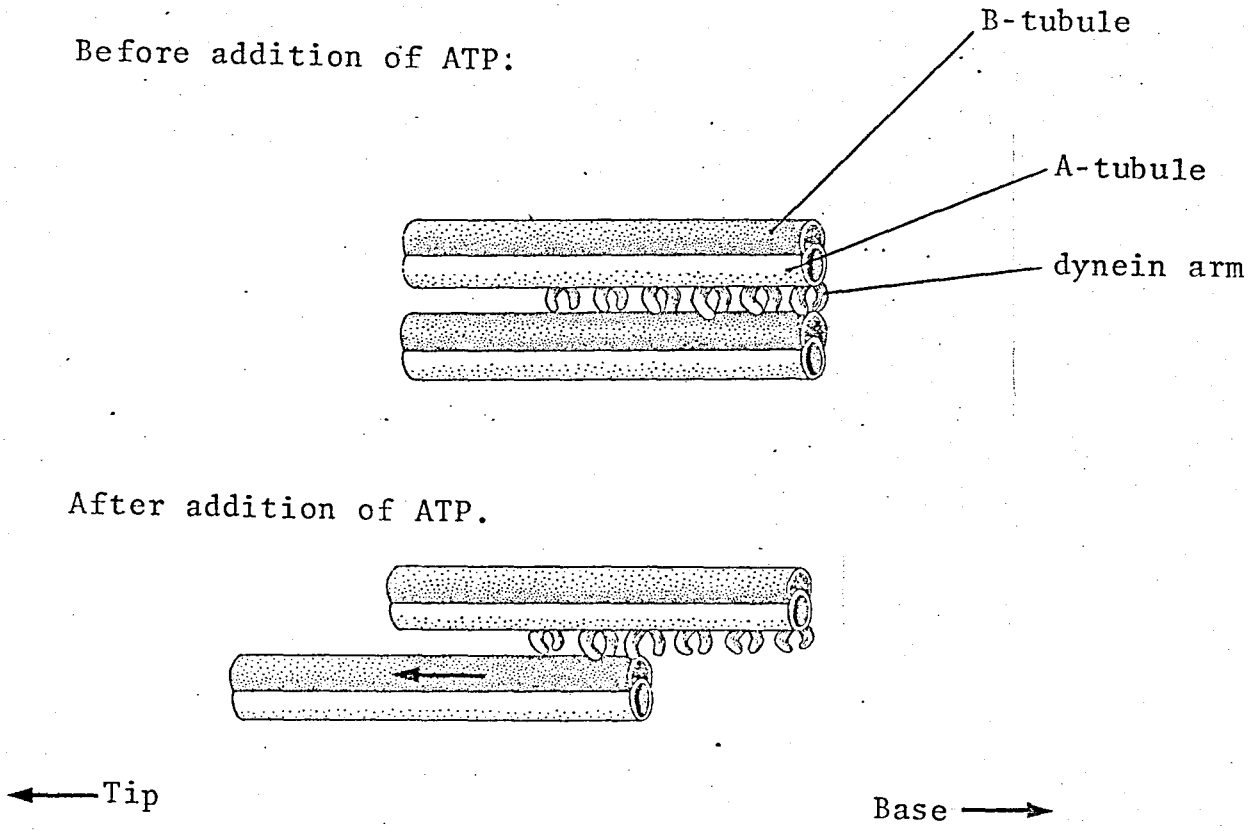

Fig. 2. The sliding-microtubule hypothesis. In an intact cilium, structures attached to the microtubules, in particular the radial spokes, resist the sliding to produce local bending. In the experiments of Summers and Gibbons (25), these structures are destroyed by trypsin treatment.

ing hypotheses have been proposed for the mechanisms of attachment and detachment of the dynein arm and the B-tubule. Gibbons and Gibbons (29) and Gibbons (30) found that abrupt removal of ATP from beating axonemes set them into stationary rigor waves due to the presence of dynein arms forming numerous cross-bridges between the doublet tubules. Thus, they concluded that cross-bridges between an A-tubule and its adjacent B-tubule are formed by the dynein arms in the absence of ATP. On the other hand, Warner and Mitchell (31) supposed that the cross-bridge was formed in the presence of ATP on the basis of observations on actively disintegrating cilia from Tetrahymena by negative contrast electron microscopy (cf. "DISCUSSION").

In the first half of the present paper, I will clearly show the mode of attachment of dynein arms to the B-tubule and their ATP-induced detachment in cilia from Tetrahymena pyriformis. Negative contrast electron microscopy showed that purified 30s dynein binds to both A- and B-tubules of outer doublets deficient of arms (EDTA-extracted outer doublets). The arms along both tubules were found at about 23 nm intervals, and were predominantly pointed toward the base at an angle of 50-55°. I found that an ATP addition caused dissociation of the arms bound to the B-tubules but not those bound to the A-tubules. In trypsin [EC 3.4.21.4]-treated axonemes, the arms were dissociated from axonemes by the addition of ATP and the turbidity of the axonemal suspension was decreased. From the similarity of the dependence of the ATPase activity and the turbidity change of trypsin-treated axoneme on ATP concentration, I concluded that dissociation of the dynein arms from the B-tubule was induced by the binding of ATP to the

active site of dynein ATPase.

Therefore, it might be expected that the A-tubule, the B-tubule, and dynein arms are functionally analogous to the core of the thick filament composed of light mero-myosin, the thin filament of F-actin, and projections of the thick filament composed of heavy mero-myosin, respectively. However, the description of the dynein molecule (16,32) and three to four subunit arms (16) showed that dynein is not structurally analogous to the muscle protein myosin, which is known to be a double-headed rod-like protein having two hinge-regions (33) (see Table II).

In the latter half of this paper, I examined the kinetic properties of dynein ATPase to clarify the differences and similarities between the dynein-tubulin system and the myosin-actin system. I found that dynein ATPase shows an initial burst of P_i liberation like myosin ATPase (34). I also found that in dynein-tubulin system, 2'-dATP and 3'-dATP can but ε ATP and FTP can not be substituted for ATP, although in the myosin-actin system all these ATP analogs can be substituted for ATP (35-37).

A molecular model for the active sliding between doublet microtubules is postulated on the basis of the findings in this study.

EXPERIMENTAL PROCEDURE

Tetrahymena pyriformis, strain W, was obtained from a stock maintained by Dr. K. Kuroda at the Department of Biology, Osaka University. The cells were grown in 2% polypeptone, 1% glucose, and 0.2% yeast extract at pH 7.3. After 4 days, the cells were harvested in a continuous flow centrifuge at 950 x g.

The cilia were isolated by the ethanol-calcium procedure used by Gibbons (7), except that the final $CaCl_2$ concentration was raised to 20 mM. Cilia and axonemes were kept at 0-4°C. Isolated cilia were sedimented at 11,000 rpm for 15 min in a Sorval SS34 rotor, and suspended in a buffer (referred to as "suspension solution" hereafter) containing 25 mM KCl, 2.5 mM $MgSO_4$, 0.2 M sucrose, 1 mM DTT, and 30 mM Tris-HCl at pH 8.3. Finally, the suspension of cilia was centrifuged at 3,000 rpm for 5 min to remove a small number of contaminating cell bodies. The cilia were mixed with an equal volume of the suspension solution containing 1% (v/v) Triton X-100 (Wako Pure Chemical Co., Tokyo). After 7-10 min, axonemes were sedimented by centrifugation at 11,000 rpm for 5min, and the axonemal pellet was resuspended in the suspension solution, using a "Komagome" pipette. Axonemes were immediately washed with the suspension solution by centrifugation, and stored in an ice bath.

The 30s dynein and outer doublets deficient in dynein arms were prepared by a modification of the method of Gibbons (9). The axonemal suspension was dialyzed against 0.1 mM EDTA, 1 mM DTT, and 1 mM Tris-HCl at pH 8.3 overnight, followed by centrifugation twice at 11,000 rpm for 15 min. The precipitate, i.e.,

EDTA-extracted doublets, was resuspended in the suspension solution, and stored in an ice bath. The supernatant was concentrated by ultrafiltration through a Toyo ultrafilter (UK 50), layered on top of a 5 to 30% (w/v) sucrose gradient in 0.5 mM EDTA, 1 mM DTT, and 5 mM Tris-HCl at pH 8.3, then centrifuged for about 18 h at 25,000 rpm in the SW 25.1 rotor of a Beckman model E centrifuge. The 30s dynein fraction was dialyzed against 2.5 mM $MgSO_4$, 0.2 mM EDTA, 1 mM DTT, and 30 mM Tris-HCl at pH 8.3, and stored in an ice bath.

KCl-extracted dynein was prepared as follows. Axonemes were suspended in 2.5 mM $MgSO_4$, 0.2 mM EDTA, 0.5mM DTT, and 30 mM Tris-HCl at pH 8 (referred to as "standard buffer" hereafter) plus 1 mM ATP. The suspension was mixed with an equal volume of the standard buffer containing 1 M KCl at 0°C. After 4 min, the suspension was centrifuged at 15,000 rpm for 5 min in a Sorval SS34 rotor. The obtained supernatant and precipitate were used as the KCl-extracted dynein fraction and the tubule fraction, respectively. The axonemes and both of dynein were used within a week after preparation.

The Triton model of Tetrahymena was prepared by the method of Naitoh and Kaneko (38), except that the concentration of Triton X-100 was 0.04% and the extraction time was a few minutes. The bending movement stopped immediately on addition of 0.04% Triton-X-100.

Pyruvate kinase [EC 2.7.1.40] was prepared from rabbit skeletal muscle by the method of Tiez and Ochoa (39). The ATP analogs (36) except AMPPNP, were kind gifts from Dr. H. Takenaka of this laboratory. ATP was obtained from Kohjin Co., Tokyo. AMPPNP was

obtained from Sigma Chemical Co., St. Louis, MO. [δ-^{32}P]-ATP was prepared enzymatically by the method of Glynn and Chappell (40). PEP was obtained from Sigma Chemical Co.

SDS-gel electrophoresis was performed by the method of Weber and Osborn (41) with slight modifications (42). Before being applied to a gel, the samples were dialyzed against 2% SDS, 1 mM EDTA, and 10 mM sodium-phosphate buffer at pH 7.0 overnight. The gel contained 3.5% acrylamide, 0.095% methylene-bis(acrylamide), 0.1% SDS, and 50 mM phosphate buffer at pH 7.3. After electrophoresis, the gel was stained at 45°C for 1 h with 0.2% Coomassie brilliant blue. Electrophoretograms were scanned with a densitometer from Fuji Riken Co. (Tokyo) at a wavelength of 570 nm.

Axonemes (0.6 mg/ml) were digested with 1.2 µg/ml trypsin (Worthington Biochemical Corporation) in the presence of 2.5 mM $MgSO_4$, 0.2 mM EDTA, 1 mM DTT, and 30 mM Tris-HCl at pH 8.3 and 20°C. The extent of digestion was estimated by turbidimetry. The digestion process was halted by adding excess soybean trypsin inhibitor (Sigma Chemical Co.) and the digested axonemes, kept in an ice bath, were used immediately.

All the experiments were performed at 20°C in standard medium containing 2.5 mM $MgSO_4$, 0.2 mM EDTA, 0.5 mM DTT, and 30 mM Tris-HCl (pH 8), unless otherwise stated. When the pyruvate kinase system was coupled with dynein ATPase, 5 mM KCl was added to the standard solution. ATPase activity was determined by determining the amount of Pi or ^{32}Pi liberated using ATP or [γ-^{32}P]-ATP as substrate after stopping the reaction with TCA, as described previously (43). When pyruvate kinase was used as an ATP-regenerating system, the ATPase activity was determined in the standard

buffer plus 0.1 mg/ml pyruvate kinase, 1 mM PEP, and 5 mM KCl by measuring the time-dependence of pyruvate-liberation by the method of Reynard et al. (44,45).

To measure the extent of activation of dynein ATPase with the tubules, the KCl-extracted dynein fraction was mixed with a suitable amount of the tubule fraction, and dialyzed against the standard buffer for more than 2 h. The extent of dissociation of dynein arms from the B-tubule was estimated from the turbidity change induced by NTP of the suspension of axonemes digested with trypsin for 5 min at 20°C, as described above. Turbidity at 350 nm was measured using 1-cm cuvettes, with or without a 7-mm spacer in a Hitachi 200-10 spectrophotometer at 20°C.

Axonemes were observed with a microscope (Zeiss Photo II) with a 40X 1.00NA objective lens and dark-field illumination. The light source was an OSRAM HBO 200W unit. The active sliding of outer doublets (25,26,31) was observed using axonemes not treated with trypsin under a light microscope with dark field illumination. A small amount of axonemes suspended in the standard buffer was placed on a glass slide, then a cover slip was added. Next, a drop of 0.15 mM NTP in the standard buffer was added to the edge of the cover slip, and a piece of filter paper was put along the other edge of the cover slip. The bending movement and the reorientation of cilia were observed using the Triton model of Tetrahymena under a light microscope, as described above. The bending movement was observed in the standard buffer plus 3 mM EGTA. The reorientation of cilia (38) was observed in a medium containing 1 mM NTP, 50 mM KCl, 0.1 mM $CaCl_2$, and 10 mM Tris-maleate at pH 7.0 and 20°C.

For negative contrast electron microscopy, an axonemal suspension with or without ATP was applied to a Formvar-carbon-stabilized copper grid. After 1 min, the grid was drained but not dried by touching it to the edge of a piece of filter paper, and the specimen was negatively contrasted with 1% aqueous uranyl acetate at pH 4.5. Electron micrographs were taken with a JEM 100-C electron microscope at 80 kV.

Protein concentration was usually determined by the biuret reaction or the method of Lowry et al. (46) as modified by Bensadoun and Weinstein (47). The concentration of 30s dynein was calculated from the absorbance at 280 nm. All of these assays were standardized by the biuret procedure with bovine serum albumin as the standard.

RESULTS

[I] The Binding Properties of Dynein Arms to the A- and B-tubules of Outer Doublet of Cilia.

Binding of 30s Dynein with A- and B-tubules, and ATP-induced Dissociation of the Dynein Arm from the B-tubule ---- I observed the binding of purified 30s dynein to EDTA-extracted doublets under the standard conditions at 0°C with or without ATP by negative contrast electron microscopy. Figure 3a shows the EDTA-extracted doublets. As reported by Gibbons (6), the arms were almost completely removed from the doublets by EDTA extraction. In many axonemes, the cylindrical structure of nine outer doublets was disrupted, and several doublets were arrayed side by side. The interdoublet spacing was 11.0 ± 2.2 nm S.D. (47)*. Single doublets were also observed. The widths of two subtubules composed of the doublets were different, and their ratio was 1.30 ± 0.17 S.D. (59). In the case of the doublets dissociated from the axonemes by ATP, the A-tubule could be identified by the attached dynein arms, and the ratio of the A- to B-tubule width was 1.13 ± 0.14 S.D. (76) (cf. Fig. 12a). Therefore, I distinguished the A-tubule from the B-tubule of each doublet by their widths. In several cases, the A-tubule was also identified by attached spokes (cf. Fig. 13).

Figure 3b and c show the EDTA-extracted doublets (0.3 mg/ml)

---

* The number not underlined in parentheses represents the number of observations.

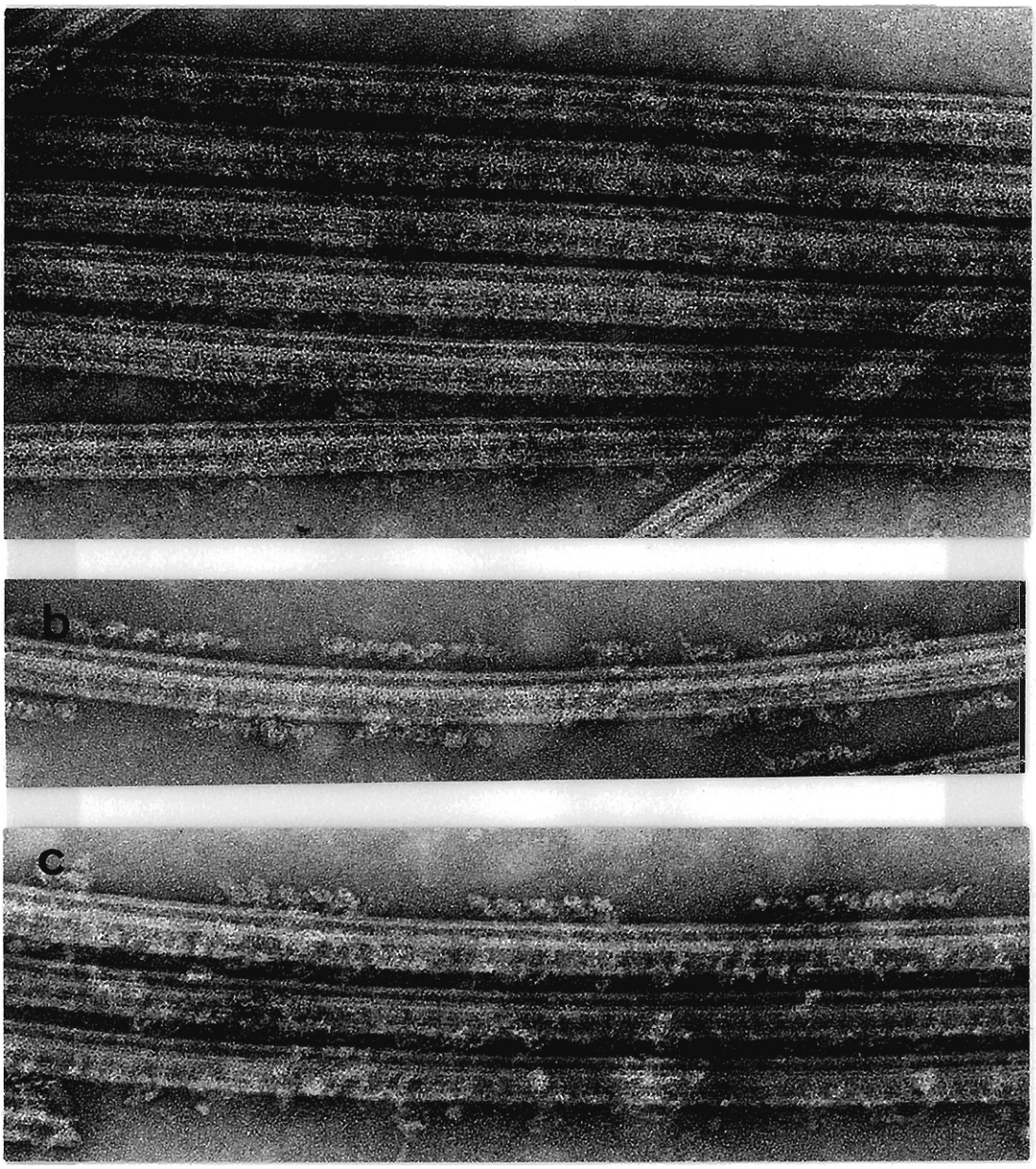

Fig.3. Negatively contrasted EDTA-extracted outer doublets of Tetrahymena cilium before and after addition of 30s dynein in the absence of ATP. 2.5 mM $MgSO_4$, 0.2 mM EDTA, 1 mM DTT, and 30 mM Tris-HCl at pH 8.3 and 0°C. The B-tubule is the upper one in each doublet. a: EDTA-extracted doublets deficient in dynein arms. b and c: Doublets (0.6 mg/ml) mixed with 30s dynein (0.038 mg/ml). Scale bar, 100 nm.

mixed with 38 μg/ml 30s dynein under the standard conditions at 0°C. The A- and B-tubules of each doublet were both decorated with an almost equal number of arms.

Figure 4 shows the EDTA-extracted doublets (0.3 mg/ml) mixed with 0.15 mg/ml 30s dynein. Figure 4a is a photograph of a single doublet, and Fig. 4b is a one-step translation of Fig. 4a. Under these conditions, rows of arms along both A- and B-tubules were observed. The profile of arms bound to the B-tubule was more distinct. Figure 4c shows three doublets arrayed side by side. Arms appeared between the doublets as well as at both edges. The interdoublet spacing was 14.1 ± 2.1 nm S.D. (93), which was about 3 nm wider than that before the addition of 30s dynein (11.0 ± 2.2 nm). I could not determine the direction of the arms located between the doublets.

Figure 5 shows the measured dimensions of the arms bound to a single doublet. The periodicity of the arms bound to the A-tubule, 22.8 ± 1.5 nm S.D. (81), was almost equal to that of the arms bound to the B-tubule, i.e., 22.5 ± 1.7 nm S.D. (61). These values agreed well with the value of 24 nm obtained by Amos et al. (48) from the optical diffraction of doublets in the absence of ATP. The lengths of the arms bound to the A- and B-tubules were almost equal, being 22 ± 3 nm S.D. (86) and 24 ± 3 nm S.D. (159), respectively. Both arms bound to the A- and B-tubules pointed in the same direction at angles of 55 ± 7° S.D. (111) and 48 ± 7° S.D. (159), respectively, and a single doublet having arms along both sides assumed an arrowhead structure.

Figure 6a shows a micrograph taken after addition of ATP to the reconstituted doublets from the EDTA-extracted doublets

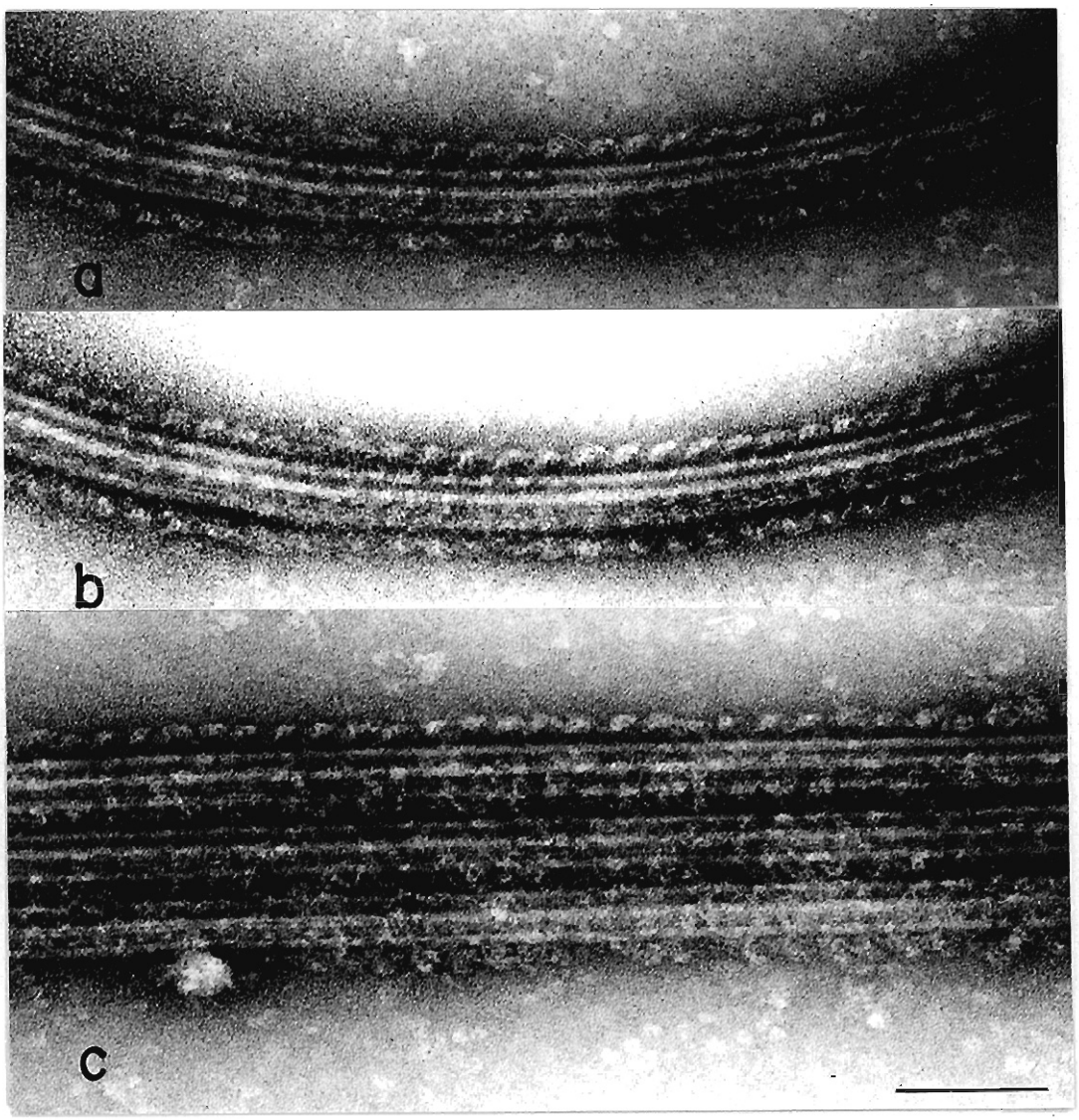

Fig. 4. Binding of dynein arms to A- and B-tubules in the absence of ATP. EDTA-extracted doublets (0.6 mg/ml) were mixed with 30s dynein (0.3 mg/ml) under the same conditions as those used in the experiments shown in Fig. 3. The B-tubule is the upper one in each doublet. a: Single doublet decorated with arms along the A- and B-tubules. b: One-step linear translation of Fig. 4a. c: Three doublets arrayed side by side and decorated with arms. Scale bar, 100 nm.

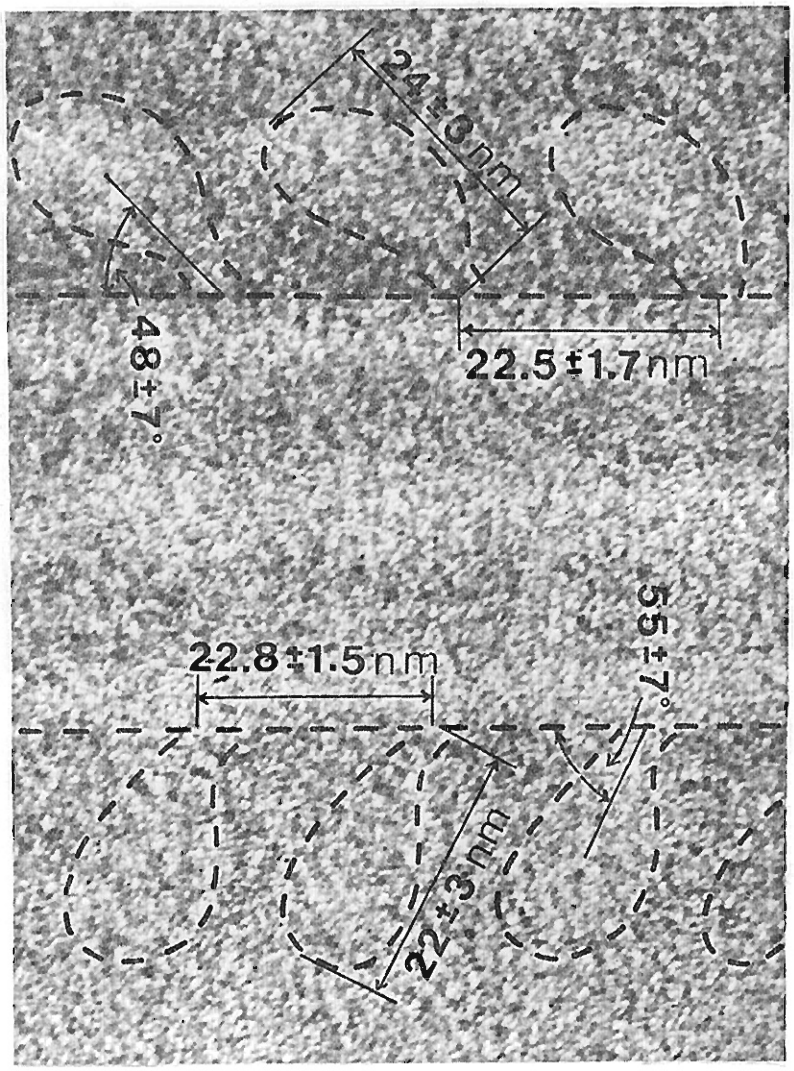

Fig. 5. Average dimensions of arms bound to a single doublet. The B-tubule of the doublet is on the upper side of the figure.

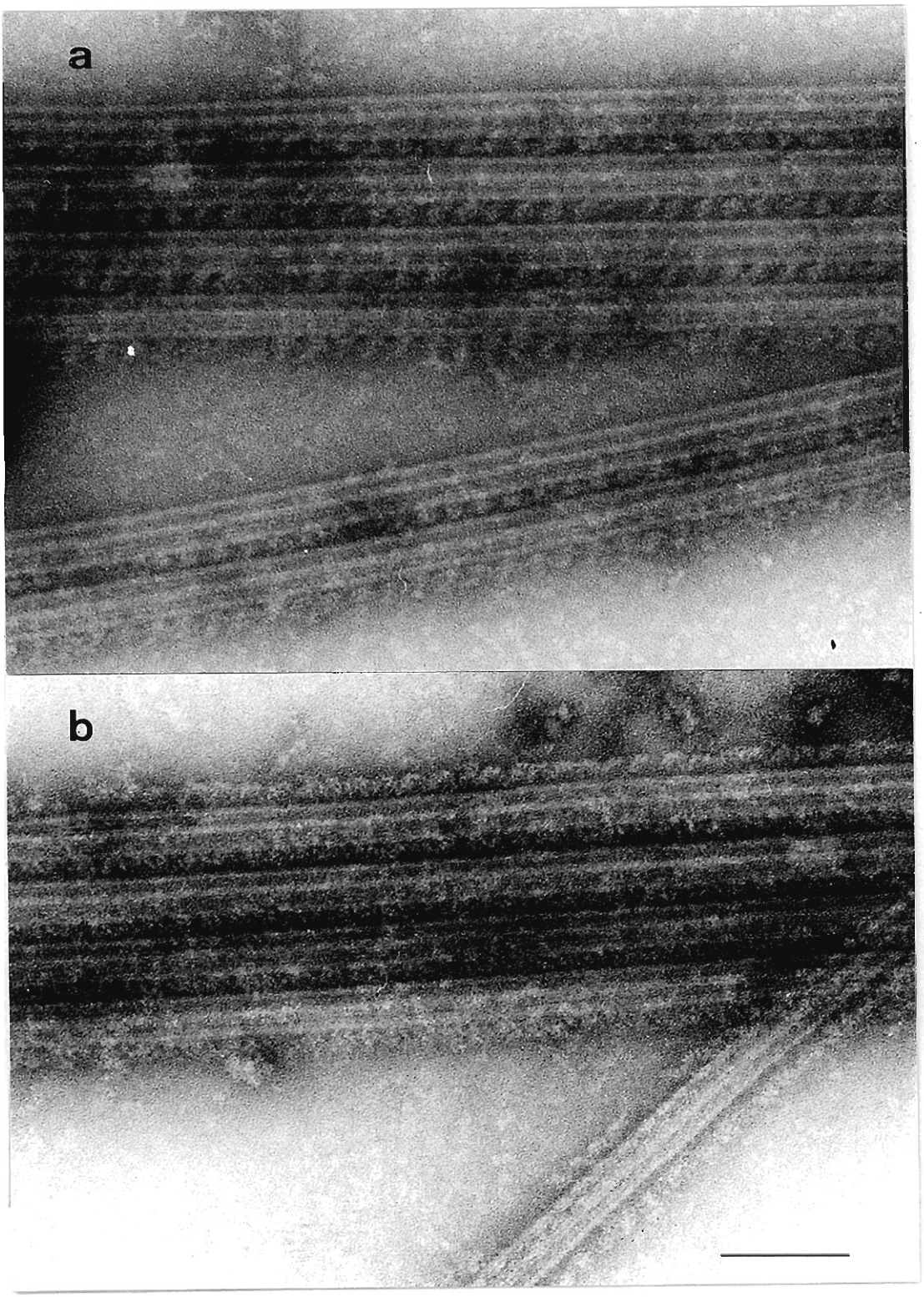

Fig. 6. Dissociation of the dynein arms from the B-tubule by ATP. Conditions were as given in Fig. 4, except for the addition of 1 mM ATP. The B-tubule is the upper one in each doublet. a: Immediately after the addition of 1 mM ATP. Notice that arms along the B-tubule were completely dissociated. b: After hydrolysis of added ATP. Notice that the arms had rebound themselves along the B-tubule. Scale bar, 100 nm.

(0.3 mg/ml) and 0.15 mg/ml 30s dynein. A row of arms appeared only along the A-tubules. The profiles of the arms bound to the A-tubule became clearer, and the angle between the axis of the arm and the A-tubule increased from 48° ± 7° to 61° ± 7° S.D. (154). The angle in the presence of ATP agreed well with the value of 58 ± 4° S.D. reported by Warner and Mitchell (31). It was remarkable that all the arms along the B-tubule became dissociated in the presence of ATP and no structure remained attached to the B-tubule. Furthermore, the interdoublet spacing was 17.3 ± 2.4 nm S.D. (56), which was 3 nm wider than that in the absence of ATP. The spacing in the presence of ATP was almost equal to the value of 16.3 ± 0.5 nm S.D. reported by Warner and Mitchell (31).

Figure 6b is a micrograph taken a few hours after the addition of ATP. A row of arms had reappeared along the B-tubules, and the interdoublet spacing had decreased from 17.3 ± 2.4 nm S.D. to 15.1 ± 2.1 nm S.D. (39).

Using doublets which slid out from demembraned axonemes, I obtained results similar to those for the EDTA-extracted outer doublets. As reported by Summers and Gibbons (25) and Sale and Satir (26), the dynein arms of these doublets were observed to bind only to the A-tubule in the presence of ATP (cf. Fig. 12a). I found that when 30s dynein was mixed with the disintegrated axonemes after hydrolysis of ATP, arms also appeared along the B-tubule. Only the arms bound to the B-tubule became dissociated by the addition of ATP, and those bound to the A-tubule remained on the doublet (data not shown).

The cross-bridge formation of the dynein arms between the A-

and B-tubules appears in Fig. 7, which shows the structure at the end of a partially disrupted demembraned axoneme in the absence of ATP. The edge of the B-tubule of the middle doublet was torn from the A-tubule, and cross-bridges seemed to be formed between the B-tubule and the adjacent A-tubule.

Disintegration of the Trypsin-treated Axoneme by ATP and Formation of Aggregates after ATP Hydrolysis ---- I digested 0.6 mg/ml of demembraned axoneme with 1.2 μg/ml of trypsin under the standard conditions at 20°C. Figure 8 shows the changes in turbidity of the axonemal suspensions digested with trypsin at various times. As already reported by Summers and Gibbons (49), Sale and Satir (26), and Witman et al. (50), the turbidity of the axonemal suspension decreased with increase in the digestion time. On adding 1 mM ATP, the turbidity of the axonemal suspension not treated with trypsin decreased very rapidly to about 80% of its initial value. The turbidity of all the digested axonemal suspensions decreased to 60% of the initial value. The time course of the turbidity change of the digested axonemal suspension was different from that of the undigested one. The turbidity of the undigested axonemal suspension from Tetrahymena could not be recovered, as reported by Gibbons (51). On the other hand, the turbidity of the digested axonemal suspension remained low for a certain period after ATP addition, then increased. The increment was constant regardless of the digestion time, and the new level was always lower than that before the ATP addition.

Figure 9 shows the time courses of turbidity change of trypsin-treated axonemal suspension after addition of various amounts of ATP. Axonemes were digested with trypsin under the conditions

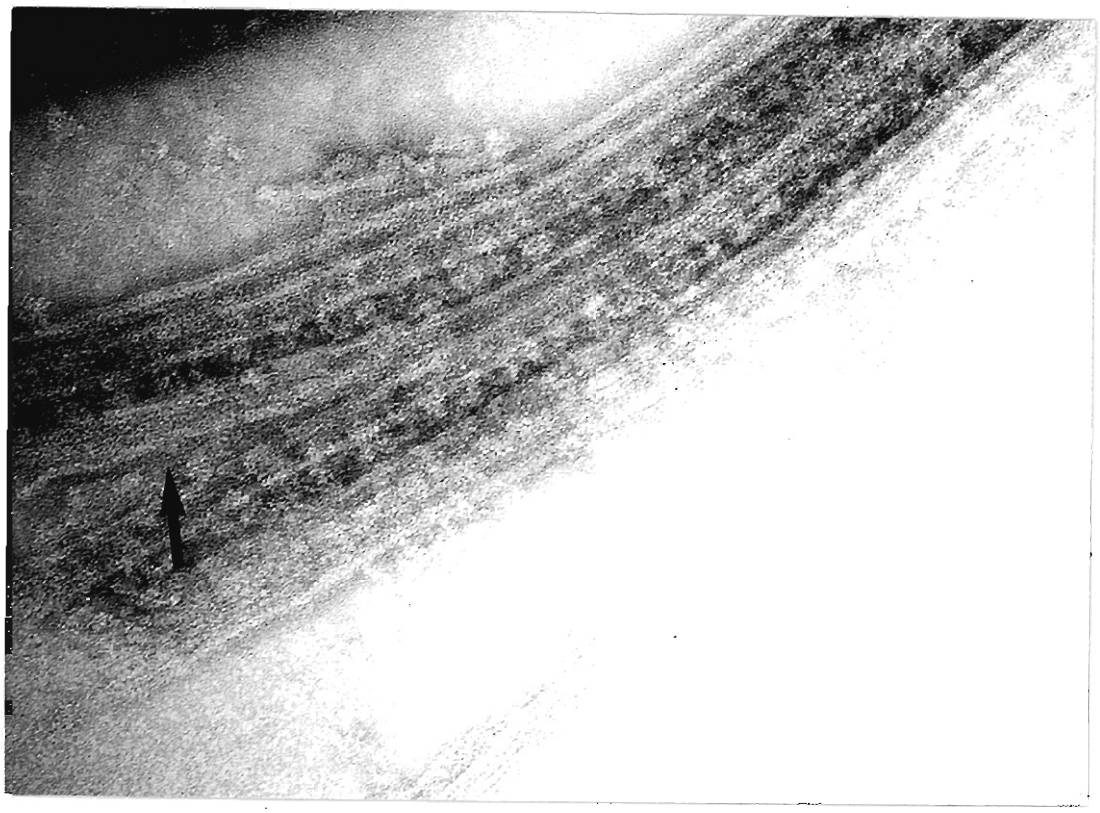

Fig. 7. Partially disrupted end of a demembraned axoneme. Notice that the edge of the B-tubule (↑) of the middle doublet was torn from the A-tubule and bound to arms along the adjacent A-tubule. The axoneme was not exposed to ATP. Scale bar, 100 nm.

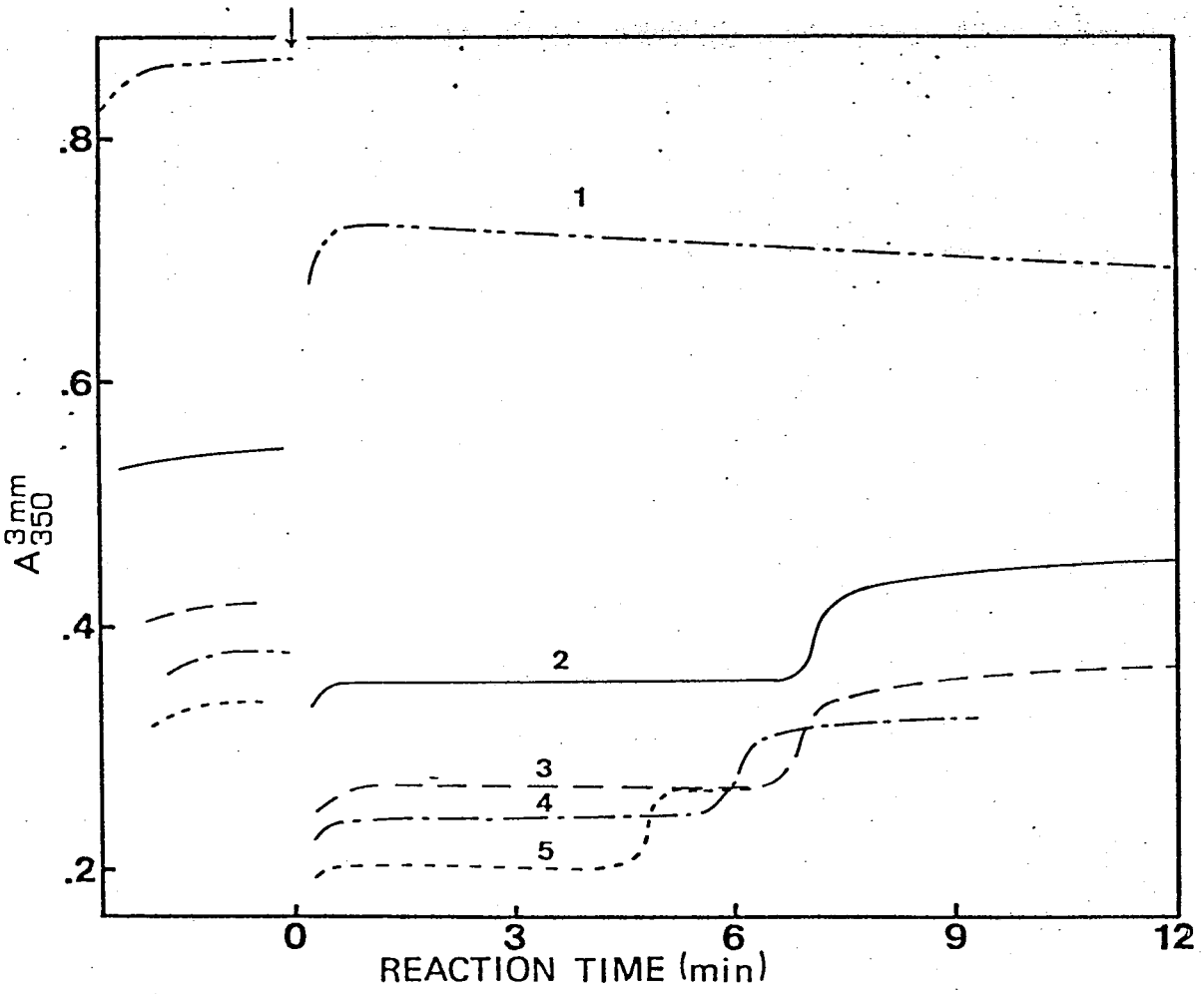

Fig. 8. Turbidity change of trypsin-treated axonemal suspension after addition of 1 mM ATP. Trypsin digestion: 0.6 mg/ml axoneme, 1.2 μg/ml trypsin, 2.5 mM $MgSO_4$, 0.2 mM EDTA, 1 mM DTT, and 30 mM Tris-HCl at pH 8.3 and 20°C for 1, 0 min; 2, 5 min 20s; 3, 8 min 50s; 4, 13 min; 5, 17 min 50s. Turbidimetry: 0.6 mg/ml trypsin-treated axoneme, 2.5 mM $MgSO_4$, 0.2 mM EDTA, 1 mM DTT, and 30 mM Tris-HCl at pH 8.3 and 20°C. The light path was 3 mm.

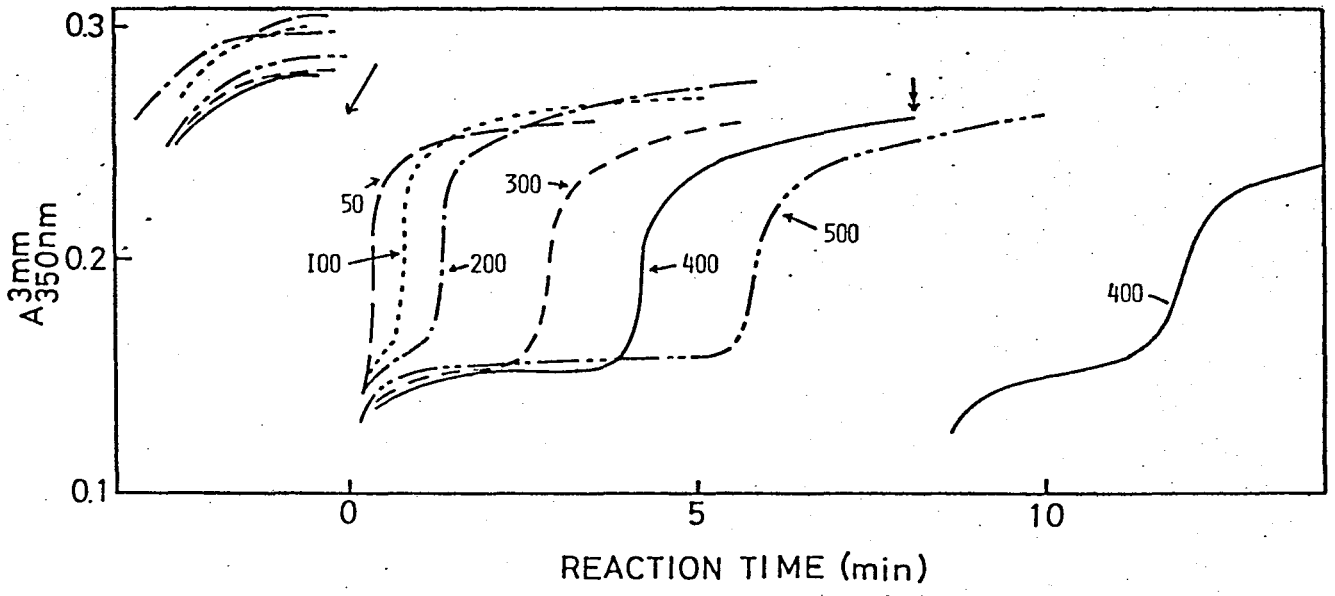

Fig. 9 Dependence of the turbidity change of the trypsin-treated axonemal suspension on ATP concentration. Trypsin digestion and turbidimetry were performed under the same conditions as the experiments shown in Fig. 8. Turbidity was decreased by trypsin digestion to about 51% of its initial value. ↓, ATP addition; ↓, ATP (400 μM) re-addition. The numbers indicate the final concentrations of ATP (μM).

used in the experiments shown in Fig. 8, and the turbidity decreased upon digestion to about 51% of its initial value. On adding ATP (50-500 μM), the turbidity dropped by 50%. The period during which the decreased level of turbidity was maintained increased with increase in the amount of added ATP. When ATP was added again (↓) after the turbidity had increased to an intermediate level, it decreased again to the low level.

Figure 10 shows dark-field photomicrographs of the trypsin-treated axonemes before and after the addition of 1 mM ATP. The turbidity of the suspension was decreased to 55% of its initial value by the digestion. Figures 10a and b show the axonemes before and just after addition of 1 mM ATP, respectively. Many axonemes disintegrated upon addition of ATP. Figure 10c is a photograph taken after the turbidity of the suspension had increased again. Large aggregates of disintegrated axonemes having diameters of several tens of μm can be seen. The aggregates disappeared on re-addition of ATP (Fig. 10d).

Figure 11 shows electron photomicrographs of the trypsin-treated axonemes before and after the addition of ATP. Axonemes were digested with trypsin for 0 (Fig. 11a), 1 (Fig. 11b), and 3 min (Fig. 11c) under the conditions used in the experiments shown in Fig. 8. The trypsin-treated axonemes retained the typical cylindrical structure in the absence of ATP. Even Tetrahymena axonemes not treated with trypsin were partially dissociated due to sliding between outer doublets on adding ATP, as reported by Sale and Satir (26) and Warner and Mitchell (31) (data not shown). Figure 11d shows a photograph of the trypsin-treated (for 3 min) axonemes taken immediately after the addition

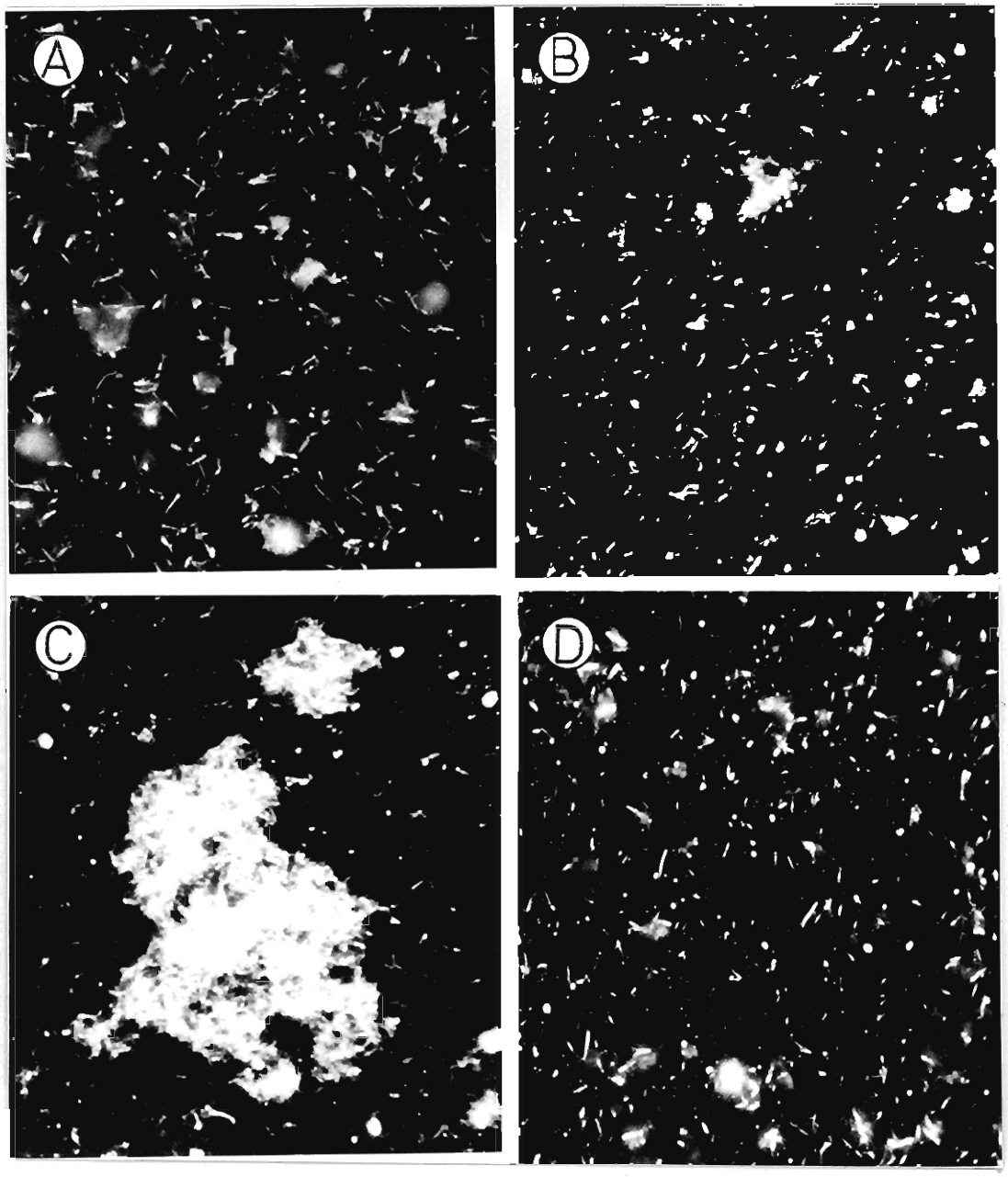

Fig. 10. Formation of aggregates of disintegrated microtubules after ATP addition, observed with a dark-field microscope. Experimental conditions were the same as those used in the experiments shown in Fig. 8. Axonemes were digested with trypsin under the conditions given in Fig. 8, and the turbidity of the axonemal suspension decreased to 55% of its initial value. a: Before addition of ATP. b: Immediately after addition of 1 mM ATP. c: 30 min after addition of ATP. d: Immediately after re-addition of 1 mM ATP. Scale bar, 10 μm.

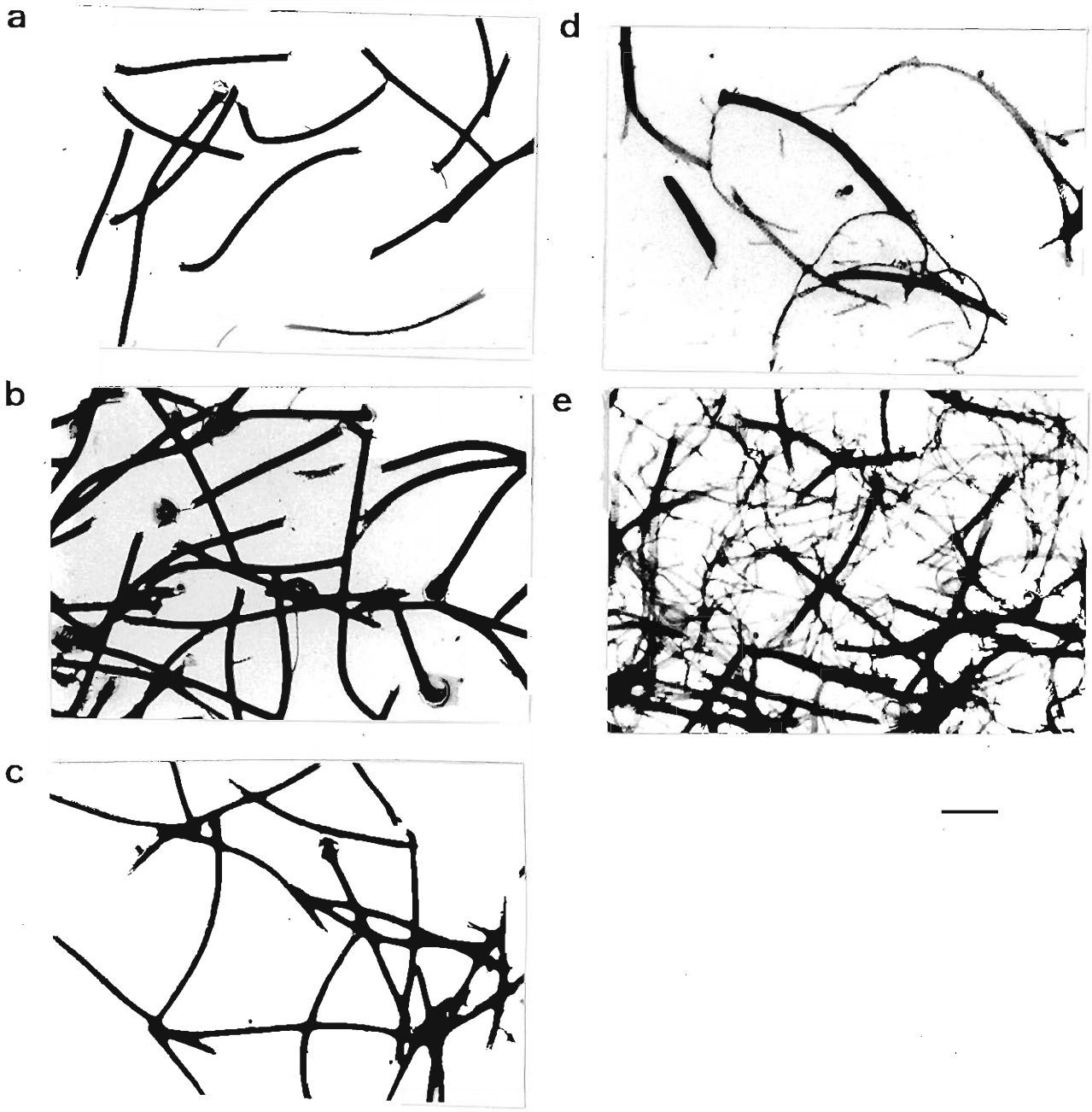

Fig. 11. Negatively contrasted trypsin-treated axonemes before and after ATP addition. Experimental conditions were the same as for Fig. 8. a: Trypsin-untreated axoneme. b: Axonemes digested with trypsin for 1 min. c: Axonemes digested with trypsin for 3 min. d: After addition of 0.3 mM ATP to trypsin-treated (3 min) axonemes. e: Trypsin-treated (3 min) axonemes after hydrolysis of the added ATP. Scale bar, 1 μm.

of 0.3 mM ATP. As reported by Sale and Satir (26), the proportion of axonemes disintegrated by ATP addition increased when they had been digested with trypsin. Figure 11e is a photograph taken after the turbidity of the suspension had increased again. Many doublets which had slid out of the axonemes formed aggregates resembling networks.

Figure 12 shows higher power images of trypsin-untreated and -treated axonemes after ATP addition. The axonemes were digested with trypsin under the conditions used in the experiments shown in Fig. 8. Figure 12a shows a portion of a trypsin-untreated axoneme disintegrated by ATP. As reported by Summers and Gibbons (25) and Sale and Satir (26), the dynein arms on the doublets were not dissociated, and appeared along the A-tubules, whereas no structure was observed along the B-tubules. On the other hand, when ATP was added to trypsin-treated (3 min) axonemes, the arms on the A-tubules were solubilized as shown in Fig. 10b. Amorphous structures remained along the A-tubule at intervals of about 99.7 ± 7.4 nm S.D. (7). The pitch was nearly equal to that of spoke repeat, i.e., 96 nm (48). Many particles that seemed to be derived from the dynein arms were observed near the doublets (↓). When the added ATP was hydrolyzed, most of the disintegrated trypsin-treated axonemes formed aggregates. Figure 12c shows a portion of the aggregates. The amorphous structures seen in the presence of ATP (cf. Fig. 12b) were also observed along the A-tubule, and a row of arms 26 ± 4 nm S.D. (71) long appeared along the B-tubule at intervals of 22.7 ± 0.7 nm S.D. (10). Both the length and interval spacing along the B-tubule were equal to those of arms bound to the B-tubule of the EDTA-extracted doublets mixed

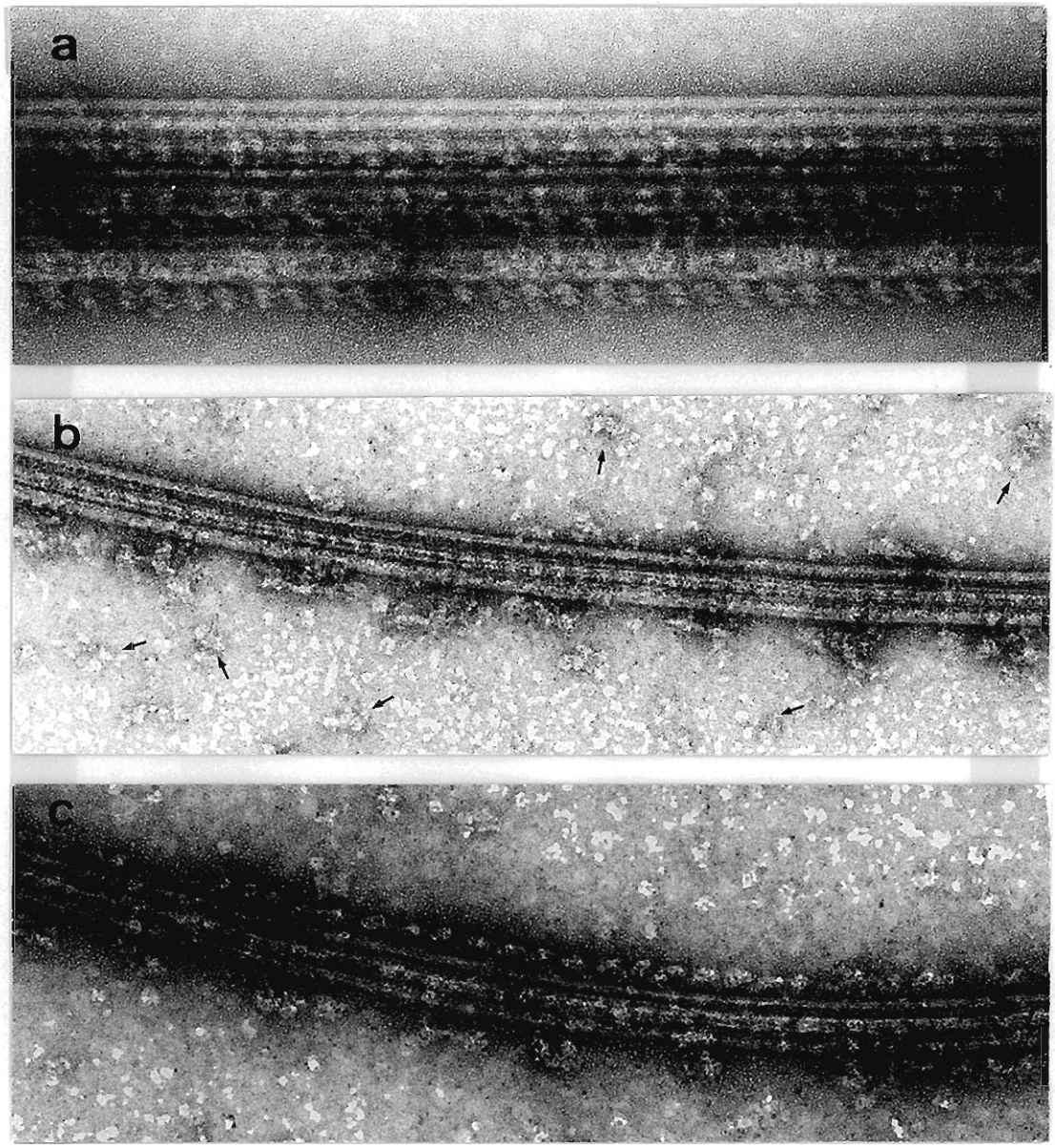

Fig. 12. Negatively contrasted trypsin-untreated and -treated axonemes after addition of ATP. Trypsin digestion and observations were performed under the conditions used in the experiments shown in Fig. 8. The B-tubule is the upper one in each doublet. a: Doublet microtubules from the ATP-disintegrated region of trypsin-untreated axoneme. b: Single doublet from ATP-disintegrated trypsin-treated axoneme in the presence of ATP. Arms solubilized from the A-tubule (↑) are seen near the doublet. c: Single doublet from ATP-disintegrated trypsin-treated axoneme after hydrolysis of the added ATP. A row of arms appeared along the B-tubule. Scale bar, 100 nm.

with 30s dynein (cf. Figs. 3 and 4).

Figure 13 is a photograph of a portion of a disintegrated trypsin-treated axoneme taken a few hours after addition of 0.4 mM ATP. In this case, axonemes (0.6 mg/ml) were digested with 0.3 µg/ml trypsin under the standard conditions at 20°C for 3 min. Triplet spoke arrangements were observed along the A-tubule (52). I could determine the basal direction of the doublet from the spoke arrangement (53), and confirmed that the arms appeared along the B-tubule pointing in the basal direction. As shown in Fig. 4, arms bound to the A- and B-tubules pointed in the same direction. Sale and Satir (26) have also shown that the arms bound to the A-tubule point in the basal direction. Thus, it is evident that the arms bound to the B-tubule tilt toward the base.

Figure 14 diagrammatically explains the phenomena observed with the trypsin-treated axonemal suspension after addition of ATP: (i) The trypsin-treated axoneme retains its structure of a cylinder with nine outer doublets in the absence of ATP, and disintegrates upon addition of ATP. (ii) Most of the arms are solubilized by the addition of ATP, and rebind to the B-tubules after hydrolysis of the ATP. (iii) Large aggregates of the outer doublets are formed when the ATP added is hydrolyzed. To explain these phenomena, I postulated that the majority of the binding sites of arms to the A-tubule were damaged by the trypsin digestion.

Dependence of the ATPase Activity and the Turbidity Change of the Trypsin-treated Axonemes on ATP Concentration ---- Figure 15 shows the dependence on ATP concentration of the rate of ATPase activity of the trypsin-treated axonemes and the extent of decrease in turbidity. The axonemes were digested with trypsin

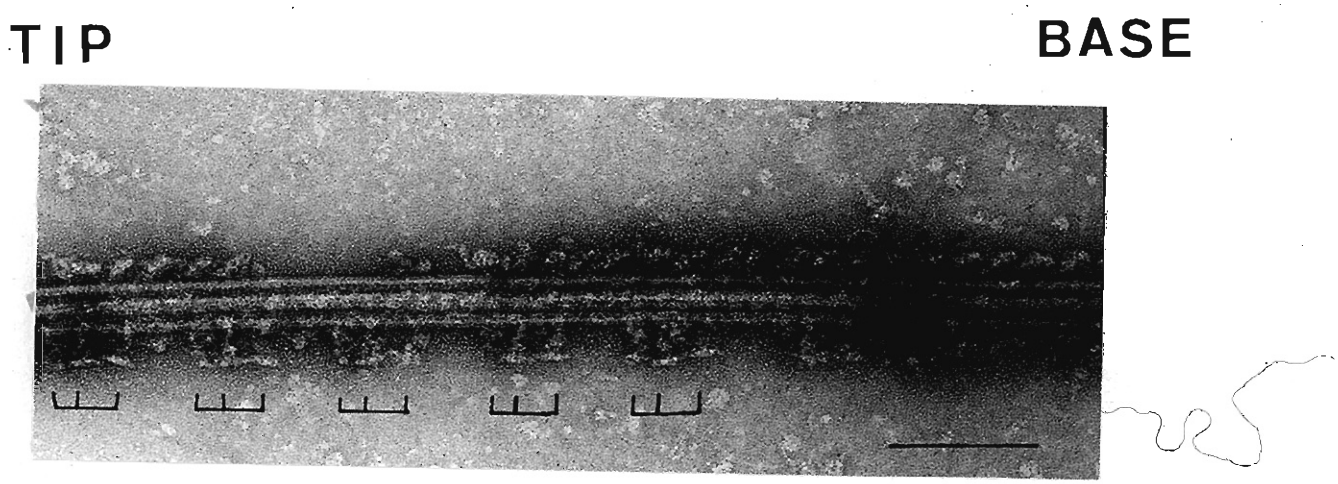

Fig. 13. Polarity of arms bound to the B-tubule. Axonemes were digested with trypsin under the conditions used in the experiments in Fig. 8 for 3 min, except that the weight ratio of axonemes to trypsin was 2,000. Axonemes were disintegrated by the addition of 0.4 mM ATP, and the single doublet obtained was stained after hydrolysis of the added ATP. The basal direction could be determined by the spoke arrangement (brackets) along the A-tubule. The dynein arms (markers along the B-tubule) tilt toward the base. Scale bar, 100 nm.

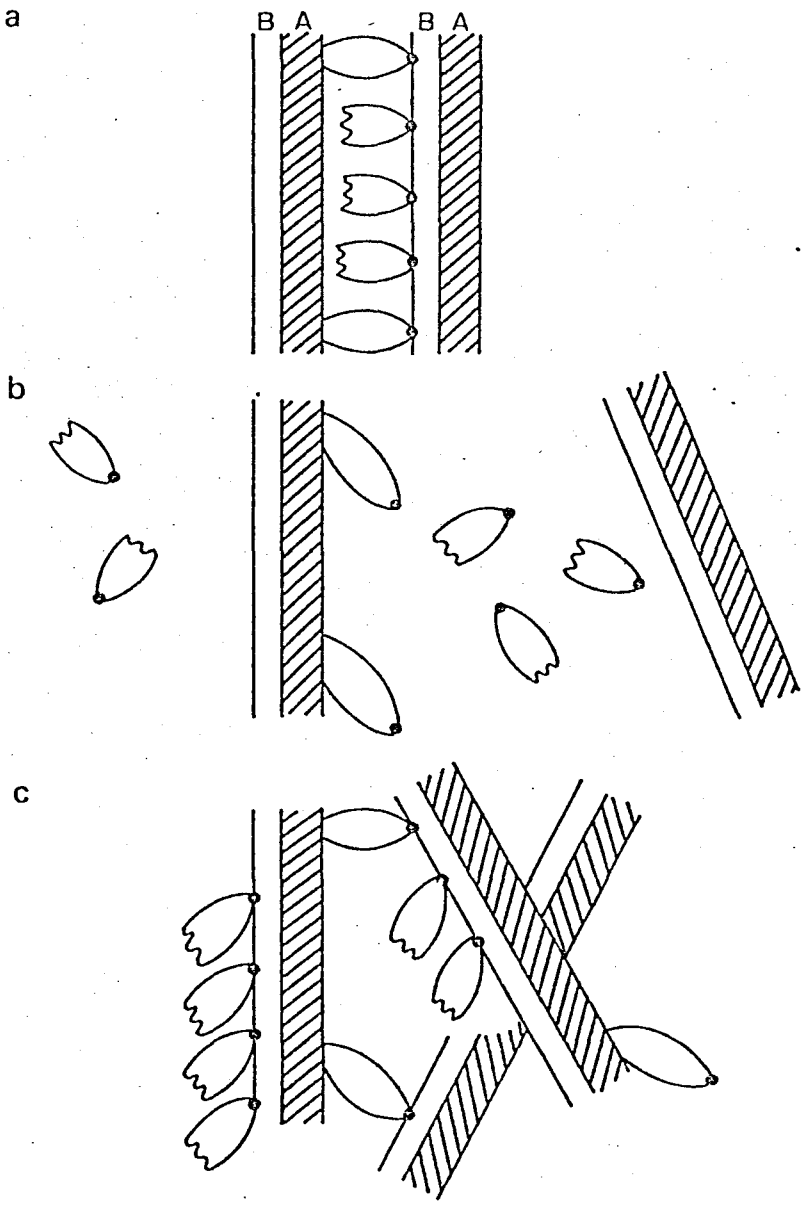

Fig. 14. A diagram to explain the phenomena observed in the trypsin-treated axonemal suspension after ATP addition. A: A-tubule. B: B-tubule. • : ATP-sensitive binding site of the arm with the B-tubule. a: Before ATP addition. For simplicity, only two of the nine outer doublets of an axoneme are shown. The binding sites to the A-tubule of many arms are digested(partially damaged arms), and a few intact arms bind to both A- and B-tubules. b: Immediately after ATP addition. Axonemes are dissociated due to the sliding induced by intact arms, and partially damaged arms are solubilized from the doublet. c: After hydrolysis of the added ATP. Partially damaged arms, which were solubilized by ATP, rebind themselves with the B-tubule. The intact arms on the A-tubule rebind themselves with the B-tubule, and large aggregates of disintegrated axoneme are formed.

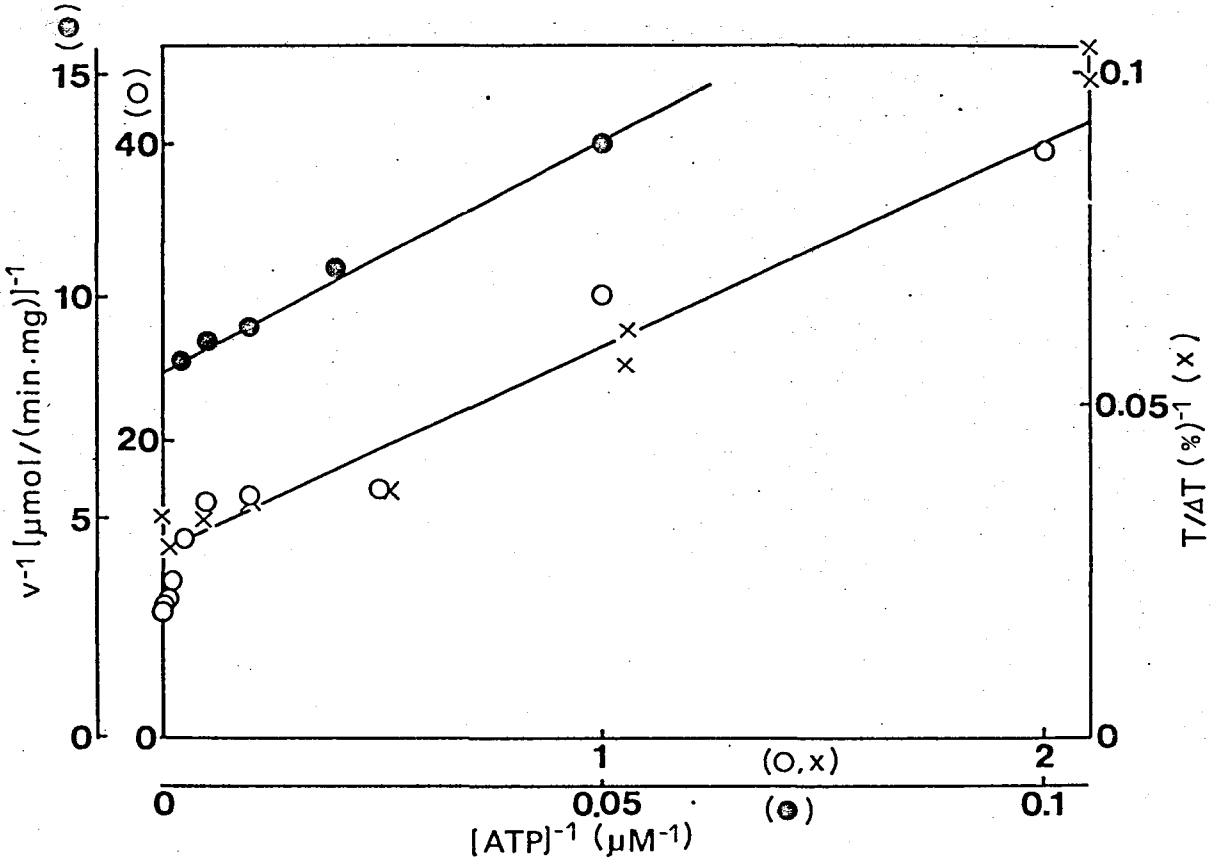

Fig. 15. Double reciprocal plots of ATPase and ATP-induced turbidity decrement of trypsin-treated axonemal suspension. The axonemes were digested by trypsin under the conditions used in the experiments shown in Fig. 8 for 3 min. ATPase activity (○, ●) and turbidity (×) were measured with 0.057 mg/ml trypsin-treated axonemes, 0.1 mg/ml pyruvate kinase, 0.5 mM PEP, 5 mM KCl, 2.5 mM $MgSO_4$, 0.2 mM EDTA, 1 mM DTT, and 30 mM Tris-HCl at pH 8.0 and 20°C. The turbidity change is given as the percentage of the turbidity decrement on ATP addition to the turbidity of the suspension before the addition.

under the standard conditions for 4 min. The ATPase activity and turbidity were measured in 0.057 mg/ml axonemes, 0.1 mg/ml pyruvate kinase, 1 mM PEP, 5 mM KCl, 2.5 mM $MgSO_4$, 0.2 mM EDTA, and 0.5 mM DTT at pH 8.0 and 20°C. The double reciprocal plot for the ATPase activity against ATP concentration was composed of two straight lines. The K_m and V_m values were 1.0 μM and 0.088 μmol/(mg.min), respectively, in the range of low ATP concentration, and were 12.7 μM and 0.12 μmol/(mg·min), respectively, in that of high ATP concentration. The double reciprocal plot for the turbidity change against ATP concentration fitted a straight line with a K_m value of 1 μM.

[II] Kinetic Properties of Dynein ATPase.

KCl Extraction of Dynein from Tetrahymena Axoneme ----Gibbons et al. reported that the ATPase activity of the dynein extracted with 0.5 M KCl or NaCl from sea urchin sperm flagella was markedly activated with microtubule protein (54). I extracted dynein with 0.5 M KCl from Tetrahymena axoneme.

About 35% of the proteins were solubilized from axonemes by extraction with 0.5 M KCl for 4 min at 0°C. Figure 16 shows the densitometer tracings of SDS gels of the supernatant (A) and the precipitate (B) from KCl-extracted axonemal solution. Thus, about 90% of the proteins with molecular weights of about 3.5×10^5 daltons were solubilized by the extraction, which accounted for about 50% of the total extracted proteins. Negative contrast electron microscopy showed that the precipitate was mainly composed of doublet microtubules deficient in dynein arms (data not shown).

Fig. 16. Densitometer tracings of SDS gels of the supernatant and the precipitate of KCl-extracted axonemes. A, supernatant; B, precipitate. 3.5% acrylamide gel was used.

The KCl-extracted dynein formed aggregates when KCl was removed by dialysis. After dialysis of the KCl-extracted dynein fraction and the tubule fraction against the standard buffer, KCl-extracted dynein became bound to the A- and B-tubules of outer doublets and formed arms along the edges, like EDTA-extracted 30s dynein, and only the arms bound to the B-tubule were dissociated from the doublet by the addition of ATP (data not shown).

Initial P_i-Burst of Dynein ATPase ---- Figure 17 shows the time courses of P_i liberation after addition of ATP to the KCl-extracted dynein fraction at 0°C. From 10 to 50 s after addition of 0.11 mM ATP, P_i was liberated linearly with time, and the extrapolated line of the plots did not pass the original point. The burst size was about 0.5 mol per 3.5×10^5 g protein. Thus, the burst size was about 1 mol per mol of 3.5×10^5 dalton proteins, since about 50% of the total extracted proteins weighed approximately 3.5×10^5 daltons.

Activation of Dynein ATPase by Binding to Ciliary Tubules ---- KCl-extracted dynein was rebound to outer doublets by dialyzing a mixture of the dynein fraction and the tubule fraction against the standard buffer at 0°C. The ATPase activities of the dynein fraction (A), the tubule fraction (B), and the mixture (C) after dialysis against the standard buffer are summarized in Table III. The activity of the rebound dynein was calculated as the difference between (C) and (B), and the value was always larger than that of dynein alone (A). The ratio of (C-B) to (A) was 1.69-1.86.

NTPase of 30s Dynein in the Steady State ---- The rates of hydrolysis of various ATP analogs by 30s dynein in the presence of Mg^{2+} are summarized in the second column of Table IV. The

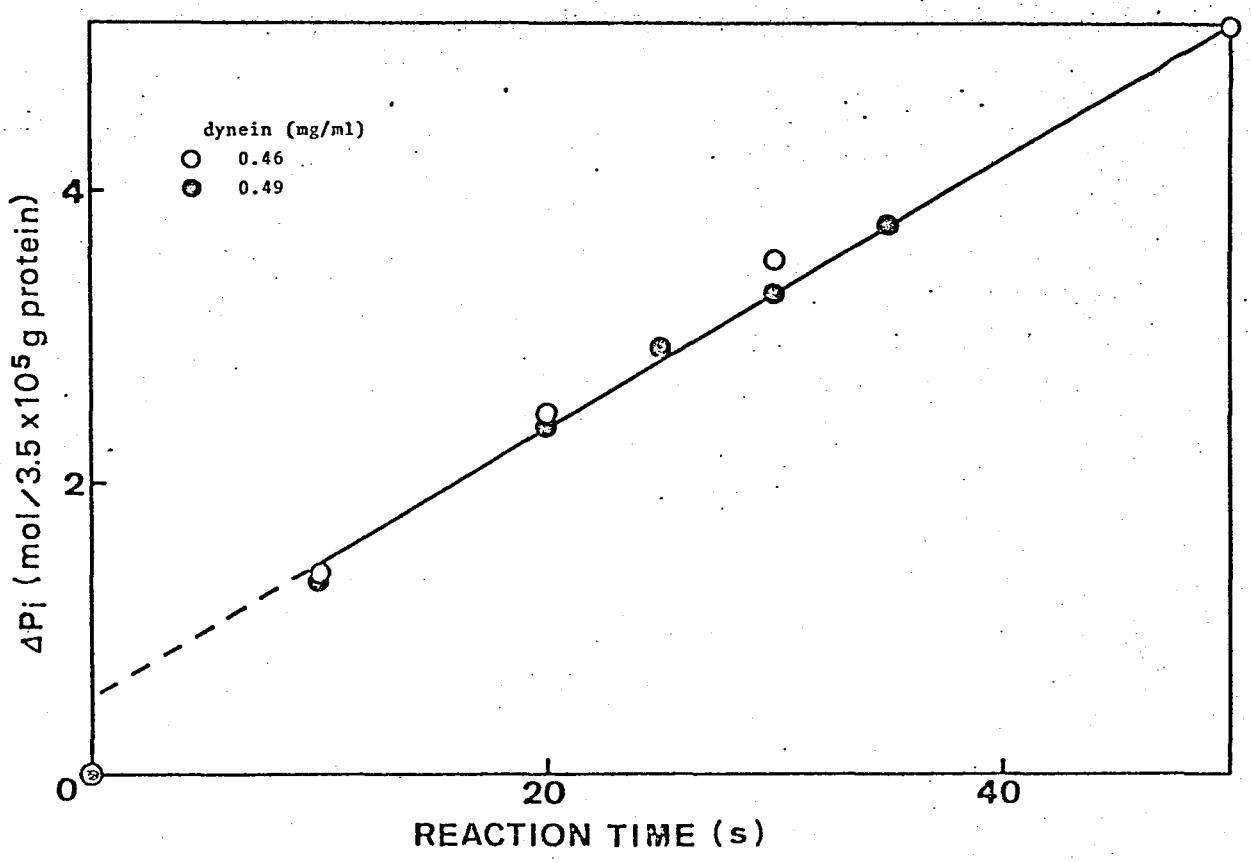

Fig. 17. Initial burst of P_i liberation of KCl-extracted dynein. 0.46 mg/ml (O) or 0.49 mg/ml (●) protein; 0.11 mM ATP, 2.5 mM $MgSO_4$, 0.2 mM EDTA, 0.5 mM DTT, and 30 mM Tris-HCl, pH 8 and 0°C. The reaction was stopped by addition of 5% TCA.

Dynein alone (A)	Tubules alone (B)	Dynein +Tubules (C)	Dynein rebound (C-B)	Activation (C-B)/(A)
64	74	193	119	1.86
49	127	212	85	1.73
35	129	188	59	1.69

Table III. Activation of dynein ATPase by ciliary tubules. Experimental conditions: 2.5 mM $MgSO_4$, 0.2 mM EDTA, 0.5 mM DTT, and 30 mM Tris-HCl at pH 8 and 20°C. ATPase activity is expressed in arbitrary units.

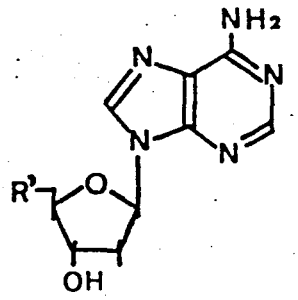

2'- dATP

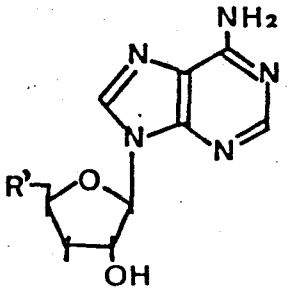

3'- dATP

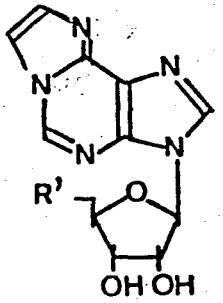

εATP

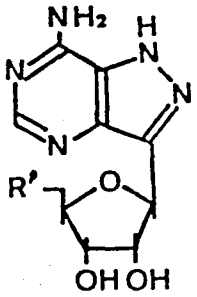

FTP

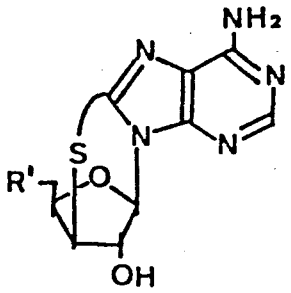

8,3'-S-CYCLO ATP

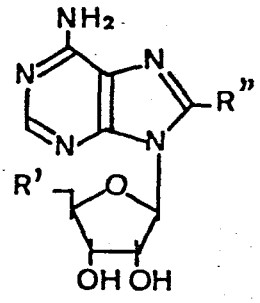

8-R ATP

R^{n} = B_R, NH·CH_3, OCH_3, SCH_3,

$$R' = -O-\left[\begin{matrix}O\\ \|\\ -P-O-\\ |\\ OH\end{matrix}\right]_3 H$$

Fig. 18. Schematic formulas of ATP analogs used in this study.

Table IV. Reaction of ATP analogs with the dynein-tubulin system. Experimental conditions: 2.5 mM $MgSO_4$, 0.2 mM EDTA, 0.5 mM DTT, and 30 mM Tris-HCl at pH 8 and 20°C. Mg^{2+}-ATPase: 0.0162 mg/ml 30s dynein, and 0.3 mM NTP, except for 0.53 mM for FTP and 0.1 mM for 8,3'-S-cyclo-ATP. Dissociation of arms: 0.06 mg/ml trypsin-treated axonemes and 30 μM NTP, except for 53 μM for FTP and 10 μM for 8,3'-S-cyclo-ATP. Sliding of outer doublets in axonemes: 0.15 mM NTP. Bending of axonemes on the Triton model: 1 mM ATP and 3 mM EGTA. Reorientation of axonemes on the Triton model: 1 mM NTP, 50 mM KCl, 0.1 mM $CaCl_2$, and 10 mM Tris-maleate at pH 7.0.

NTP	Mg^{2+}-NTPase [μmol/(min·mg)]	Dissociation of dynein arms from axonemes [ΔT/T]	Sliding movement	Bending movement	Reorientation of cilia
ATP	0.93	28	++	++	++
2'-dATP	0.96	29	++	++	+
3'-dATP	0.36	22	++	+	+
8-Br-ATP	0.43	4	-	-	-
FTP	0.29	6	-	-	-
8-$NH(CH_3)$-ATP	0.06	4	-	-	-
8-SCH_3-ATP	0.08	3	-	-	-
8-OCH_3-ATP	0.09	2	-	-	-
ATP	0	1	-	-	-
8,3'-S-cyclo-ATP	0	5	-	-	-
AMPPNP	0	3	-	-	-

activities were measured under the standard conditions in the presence of 0.016 mg/ml 30s dynein and 0.3 mM NTP, except for 0.53 mM for FTP and 0.1 mM for 8,3'-S-cyclo-ATP. The rate of hydrolysis of 2'-dATP [0.96 μmol/(min·mg)] was almost equal to that of ATP (0.93), as already reported by Gibbons (9). The rates of hydrolysis of 3'-dATP (0.36), FTP (0.29), and 8-Br-ATP (0.43) were less than 50% of that of ATP. Other ATP analogs, including εATP, which is known to be hydrolyzed by myosin more rapidly than ATP (35), were hydrolyzed at rates less than 10% that of ATP. The rate of hydrolysis of 1 μM ATP by 30s dynein was unaffected by the presence of 20 μM εATP or 10 μM 8-NH(CH_3)-ATP.

Dissociation of Dynein Arms from the B-Tubule by ATP Analogs ---- I showed in the first half of the present paper that the turbidity change of the trypsin-treated axonemal suspension caused by the addition of ATP reflects the extent of dissociation of dynein arms from the B-tubule. The extent of this dissociation induced by ATP analogs was estimated from the turbidity change of trypsin-treated axonemal suspension, and the results are summarized in the third column of Table IV. The turbidity was measured under the standard conditions at 20°C in the presence of 0.06 mg/ml trypsin-treated axonemes and 30 μM NTP, except for 53 μM for FTP and 10 μM for 8,3'-S-cyclo-ATP.

The extents of turbidity change induced by 2'-dATP (29%) and 3'-dATP (22%) were almost equal to that induced by ATP (27%). Other ATP analogs, including FTP and 8-Br-ATP, both of which were hydrolyzed by 30s dynein, induced much smaller changes in turbidity, i.e., less than 6%. Electron microscopic observation also showed that 8-Br-ATP and 8-NH(CH_3)-ATP did not dissociate

arms from the B-tubule.

Sliding and Bending Movement of Axoneme Induced by ATP Analogs ---- For many parts of Tetrahymena cilia, active sliding disintegration occurs without external proteolysis (26,31). Therefore, I observed the active sliding movement of axonemes not treated with trypsin under the standard conditions at 20°C, and the results are summarized in the fourth column of Table IV. ATP, 2'-dATP and 3'-dATP, all of which induced the dissociation of dynein arms from the B-tubule, induced active sliding between outer doublets. On the other hand, all the ATP analogs, which did not induce the dissociation, did not induce the active sliding movement.

Figure 19 shows dark-field photomicrographs of the Triton model of Tetrahymena. After treatment with 0.04% Triton X-100, both ghost models without cytoplasm (Figs. 19-3 & 19-4) and intact models (Figs. 19-1 & 19-2) were observed. The bending movement of most axonemes continued at least for 30 to 40 minutes at 20°C after addition of ATP.

As summarized in the fifth column of Table IV, 2'-dATP induced the bending movement of axonemes, as already reported by Morita et al.(55) for the Triton model of Paramecium. The extent of re-activation of 3'-dATP was very low and only a few axonemes were bent for 20 to 30 seconds. The bending movement was not observed with the addition of other ATP analogs.

Reorientation of Cilia on the Triton Model of Tetrahymena Induced by Ca^{2+} and ATP Analogs ---- Naitoh and Kaneko (38,56) showed that the direction of the power stroke of Paramecium cilia is controlled by Ca^{2+}, and concluded that Ca^{2+}-ATPase unlike

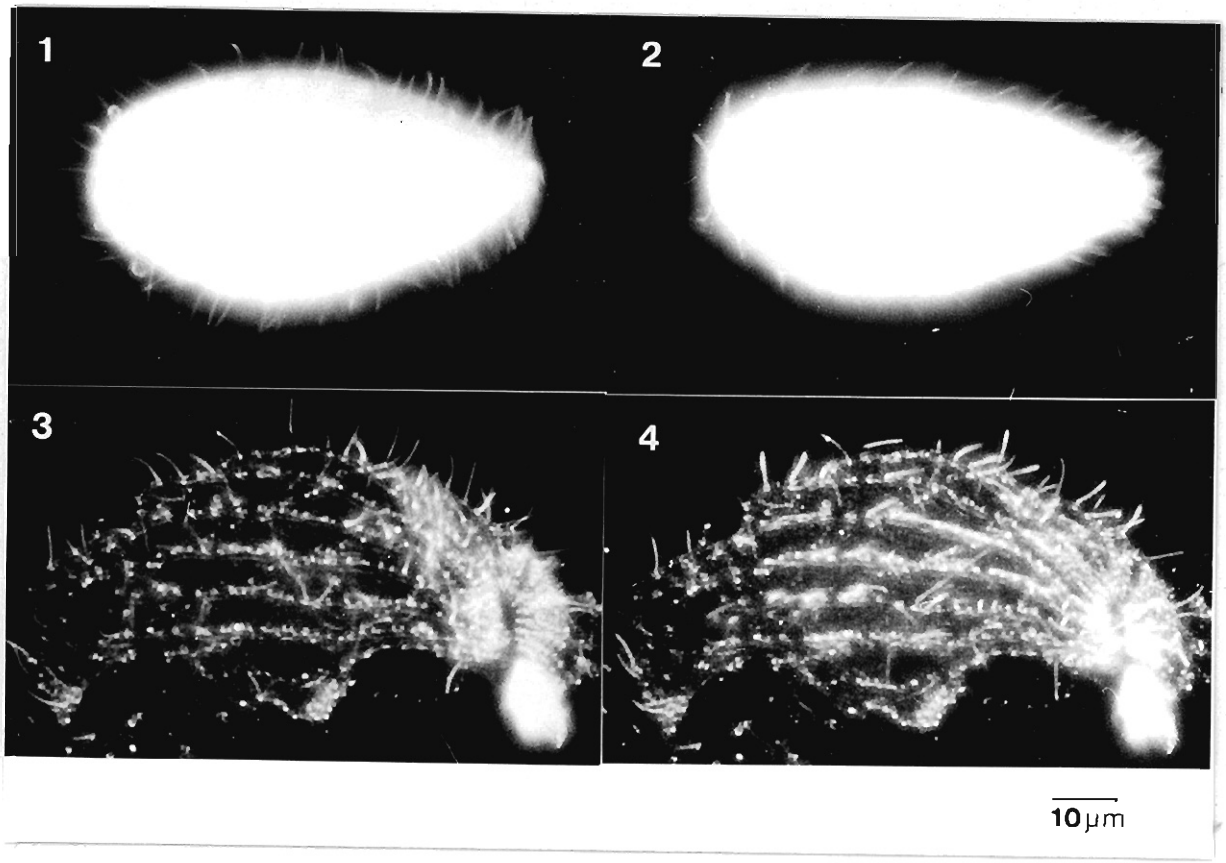

Fig. 19. Reorientation of cilia on the Triton model of Tetrahymena induced by Ca^{2+} and ATP. 50 mM KCl, 0.1 mM $CaCl_2$, and 10 mM Tris-maleate, pH 7 and 20°C. 1, 3: Before addition of ATP. 2,4: After addition of 1 mM ATP. Scale bar, 10 µm.

dynein ATPase mediates the reorientation of cilia. I examined whether ATP analogs induce the direction reorientation in the presence of 0.1 mM $CaCl_2$ using the Triton model of Tetrahymena. Figure 19 shows photographs taken before (Figs 19-1 & 19-3) and after (Figs 19-2 & 19-4) addition of 1 mM ATP in 50 mM KCl, 0.1 mM $CaCl_2$, and 10 mM Tris-maleate at pH 7 and 20°C. In the absence of ATP, many axonemes on the Triton model pointed toward the rear. On ATP addition, many beat slowly for a few seconds and shifted toward the front. This phenomenon was also observed with the "ghost model" (Figs. 19-3 & 19-4).

Figure 20 shows photographs of the Triton model in the absence (Fig. 20-1) and presence of ATP analogs (Figs. 20-2, 20-3, 20-4, 20-5, & 20-6). 2'-dATP (Fig. 20-2) and 3'-dATP (Fig. 20-3) induced reorientation of the axonemes but the rate was much slower than that induced by ATP. Other analogs did not induce the reorientation (cf. sixth column of Table IV and Figs. 20-4, 20-5, 20-6).

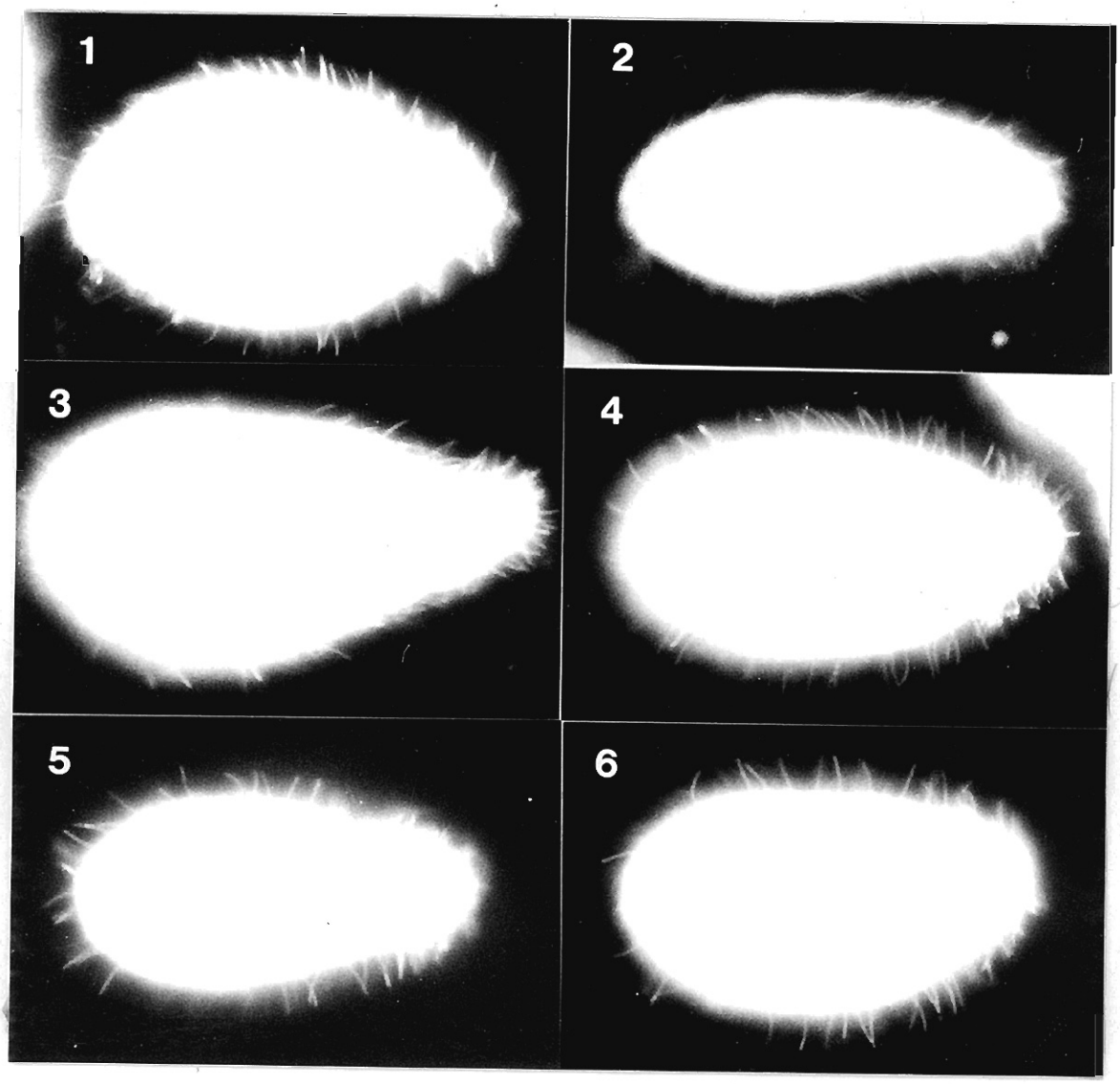

Fig. 20. Reorientation of cilia on the Triton model of Tetrahymena induced by various ATP analogs. Conditions were as in Fig. 18. 1: Before addition of NTP; 2: + 1 mM 2'-dATP; 3: + 1 mM 3'-dATP; 4: + 1 mM FTP; 5: + 1 mM 8,3'-S-cyclo-ATP; 6: + 1 mM 8-Br-ATP. Scale bar, 10 μm.

DISCUSSION

As mentioned in "INTRODUCTION," the basis of force generation of beating eukaryotic cilia and flagella is an interaction between the axonemal doublet microtubules, in which some doublets slide relative to their neighbors (24-26). However, two conflicting hypotheses had been proposed for the mechanisms of attachment and detachment of the dynein arm to the adjacent B-tubule, i.e., elementary processes required for the sliding. This study demonstrates clearly that 30s dynein can bind to both A- and B-tubules of the outer doublet to form an arm, and that ATP dissociates only the arm bound to the B-tubule.

I distinguished the B-tubule from the A-tubule of each doublet by the following criteria: (i) When negatively contrasted, the A-tubule was wider than the B-tubule, and the ratio of the width of the A-tubule to that of the B-tubule was 1.1-1.3. (ii) The characteristic arrangement of the spoke was observed along the A-tubule (52) (cf. Fig. 13). (iii) In the demembraned axoneme in which the doublets slid out on addition of ATP, there observed arms bound along the A-tubule, and the arms were not dissociated by the ATP (25,26) (cf.Fig. 12a).

The following findings excluded the possibility that arms bound to the A-tubule might have appeared as if they had been bound to the B-tubule: (i) The overall lengths of both arms bound to the A- and B-tubules were almost equal, i.e., about 23 nm. (ii) The arms appeared only along the A-tubule of the doublet which slid out from the demembraned axoneme on ATP addition (cf. Fig. 12a), unless purified 30s dynein was added.

Gibbons (6) and Shimizu (57) showed that 30s dynein when exogeneously added to axonemes deficient of arms much more strongly bound to the specific sites along the A-tubules than to non-specific sites, such binding being observed when dynein was added excessively. If the binding of arms to the B-tubules as observed in the present study had been non-specific, I would have observed arms only along the A-tubules in case a small amount of dynein was added to the doublets. But in fact the arms were almost equally formed along both the A- and B-tubules as shown in Fig. 3-b and c. Furthermore, when a sufficient amount of dynein was added to a single doublet, the periodicities of arms bound to the A- and B-tubules were almost equal. Thus the binding of arms to the B-tubules observed in this study was specific and physiological.

The finding that the spacing between doublets having arms increased on ATP addition and decreased after its hydrolysis also suggested the formation of cross-bridges between the A-tubule and the adjacent B-tubule in the absence of ATP. Thus, I concluded that a dynein arm along the A-tubule forms a cross-bridge between an A-tubule and its adjacent B-tubule in the absence of ATP, and that the cross-bridge dissociates from the B-tubule on addition of ATP, just as is observed with the myosin cross-bridge. This conclusion is consistent with the observation reported by Gibbons and Gibbons (29), that ATP induced relaxation of the rigor waves of sea urchin sperm tail.

An interaction between the dynein arms and the B-tubule was implied by the results of Ogawa (58) using a tryptic fragment of dynein (Fragment A) from sea urchin sperm tail. He showed that

the ATPase activity of Fragment A was activated by the addition of B-tubulin. Nevertheless, Fragment A did not recombine with the A-or B-tubule in the absence of ATP. Shimizu (57) reported that ATP had a strong inhibitory effect on rebinding of dynein with outer doublets, but he did not show which of the rebindings of dynein with A- or B-tubule is inhibited by ATP. Based on negative contrast electron microscopy results, Warner and Mitchell (31) suggested that cross-bridge formation by the dynein arm between an A-tubule and its adjacent B-tubule did not occur in the absence of ATP, and that the presence of ATP was required to preserve the attachment of the terminal subunit of the dynein arms to the B-tubule of Tetrahymena cilia, thus proposing that the arm assumes what they called a "bridged conformation" in the presence of ATP. They thought this conformation indicated cross-bridge formation between a B-tubule and the dynein arm fixed along the adjacent A-tubule. However, they could not establish whether the arms in the "bridged conformation" are actually bridged to the B-tubule or simply in the proximity of the B-tubule. They used the following criteria to judge whether or not the arm was bridged to the B-tubule: (i) The doublet microtubules are free to slide apart and usually do in the presence of ATP, apparently having lost the constraints that otherwise hold them together. (ii) The interdoublet spacing is uniform and does not exceed 16.3 nm, which is somewhat less than the length of the unbridged arms. (iii) Images are seen where the arms remain attached to protofilaments that have been pulled out of the B-tubule. (iv) Arms having the bridged conformation are never seen in cilia that have not been exposed to ATP.

However, their criteria (i) and (ii) can be explained easily by the presence of the nexin link. Sale and Satir (26) showed that some axonemes of Tetrahymena cilia were disintegrated by the addition of ATP without prior trypsin treatment. Some of the nexin links of Tetrahymena cilia were probably destroyed by mechanical damage or proteolysis during preparation. However, as reported by Sale and Satir (26), the percentage of disintegrated axonemes with ATP addition without prior trypsin treatment was less than 40. On the other hand, most of the cylindrical arrangement of the nine outer doublets was disrupted, and smaller groups of doublets were arrayed side by side in the case of EDTA-extracted axonemes, which were deficient in dynein arms (cf. Fig. 3a). The interdoublet spacing was uniform (11.0 ± 2.2 nm). These results indicate that many nexin links of Tetrahymena cilia remained intact, and that the dominant structure causing the array of doublets side by side in the presence of ATP was the nexin link, not cross-bridge. Also, I obtained an image resembling their "bridged conformation" in the absence of ATP, as shown in Figs. 6 and 7.

Quite recently, Warner (59) also reached the same conclusion as mine that dynein arms form cross-bridges between A- and B-tubule only in the absence of ATP from the observation of thin sections of Unio gill cilia.

The reason why the binding properties of dynein arms to the A- and B-tubule are different from each other is not yet known. I showed that a fragment of the arm which can bind only to the B-tubule is obtained by tryptic digestion of demembraned axonemes (cf. Figs.12 and 13). This fragment was different from the Fragment A obtained by Ogawa (58) from sea urchin dynein and the

12s fragment obtained by Hoshino (60) from Tetrahymena 30s dynein, as it could bind to the B-tubule. This fragment is expected to be a useful tool for studying the nature of binding sites of the arm to the A- and B-tubules and the substructure of the dynein arm.

As mentioned in "RESULTS," the change in turbidity of the trypsin-treated axonemal suspension caused by the addition of ATP supposedly reflects the dissociation of dynein arms from the B-tubule. The apparent dissociation constant (1 μM) of ATP binding to dissociate dynein arms from the B-tubule, estimated from the turbidity change, was almost equal to one of the K_m values of the ATPase reaction. This result is consistent with that of Gibbons and Gibbons (29), in which relaxation from the rigor wave was induced by 1 μM ATP. Therefore, it is reasonable to assume that the site for ATP binding which induces dissociation of the arms from the B-tubule is the same as the active site of dynein ATPase. However, Warner et al.(16) showed that the dynein arm was composed of at least three subunits, and it has been suggested that two ATP molecules are hydrolyzed per beat cycle for each dynein arm (27). Therefore, the interaction between ATP and subunits of the arm must be more complicated than is discussed here.

There has been no detailed study on the reaction mechanism of dynein ATPase. In this study, I found an initial burst of phosphate liberation in the KCl-extracted dynein ATPase reaction. This suggests that an acid-labile enzyme-phosphate complex is formed during the dynein ATPase reaction (34). Warner et al.(16) showed that the dynein arms consist of three to four morphologi-

cally similar subunits. About 90% of the proteins with a molecular weight of about 3.5×10^5 were extracted by 0.5 M KCl (Fig. 16), and the burst size of P_i liberation of KCl-extracted dynein was about 1 mol per mol of 3.5×10^5 dalton proteins (Fig. 17). These results suggest that the subunits are identical with respect to the ATPase. Nakamura and Masuyama (61) reported the initial burst of P_i liberation using dynein ATPase from Mytilus gill cilia.. However, the burst size they observed was more than 30 mol per mol of 3.5×10^5 proteins, and could not be due to the formation of an enzyme-phosphate complex.

The activation of dynein ATPase from Tetrahymena with the microtubular proteins has been already reported by Otokawa (62) and Blum and Hayes (63), but the extent of activation was less than 50%. Ogawa (58) observed the activation of ATPase activity of the tryptic subfragment of sea urchin dynein with tubulin, but not the activation of intact dynein ATPase with tubulin. The activation of dynein ATPase from Tetrahymena with brain tubulin was observed by Hoshino (64) under alkaline but not under neutral conditions. Recently, Gibbons and Gibbons (21) reported that the motility of sea urchin sperm flagella was recovered by rebinding KCl-extracted dynein to doublets. Gibbons et al.(54) showed that the ATPase activity of NaCl-extracted dynein was enhanced four- to ten fold times by rebinding to the outer doublets. I showed in this study that the ATPase activity of KCl-extracted dynein from Tetrahymena cilia increased by 70-90% by rebinding to the doublets. Thus, it is reasonable to conclude that microtubule proteins accelerate the decomposition of an intermediate of dynein ATPase $E_p^{(ADP)}$, as F-actin accelerates the decomposition of the

myosin-phosphate-ADP complex, M_P^{ADP} (34).

The dynein-tubulin system is very specific for ATP, and CTP, GTP, UTP and ITP do not induce the active sliding of outer doublets, the bending movement of axonemes, and the relaxation from "rigor waves" (9,10,18,25,29). Morita et al.(55) reported that 2'-dATP did but trinitrophenyl-ATP and εATP did not induce the bending movement of cilia on the Triton model of Paramecium. In this study, I examined the reaction of the ten ATP analogs listed in the first column of Table II with the dynein-tubulin system, and found that the system is very specific to ATP and only 2'-dATP and 3'-dATP can be substituted for it. I found that the dynein-tubulin system differs from the myosin-actin system in that the former can not use εATP and FTP as substrate (cf.35-37). Thus, FTP and 8-Br-ATP were hydrolyzed by 30s dynein faster than 3'-dATP, but they did not induce the dissociation of dynein arms from the B-tubule and the sliding movement between outer doublets. 3'-dATP was hydrolyzed by 30s dynein more slowly than ATP and 2'-dATP. Although it induced the sliding movement, it rarely induced the bending movement of axonemes.

I have no direct information as to the conformational change of the dynein arm induced by ATP at this stage, but our observations imply that the force which generates the sliding between doublets may have originated from the formation of the cross-bridge itself, since the arms bound to both the A- and B-tubules were tilted towards the base and the angles between the long axis of these arms and the A- and B-tubules were 55° and 48°, respectively. Therefore, formation of the cross-bridge probably imposes a stress on the arm fixed along the A-tubules of the nine doublets which

maintain a cylindrical arrangement, and this stress induces the sliding (cf. Fig. 21). According to this hypothesis, dynein arm slides the adjacent doublet to the top of the axoneme. This is consistent with the finding by Sale and Satir (26).

Figure 22 shows a simplest working hypothesis for the molecular mechanism of active sliding between doublets of eukaryotic cilia and flagella: (i) When ATP bound to the arm is hydrolyzed by dynein ATPase, the arm attaches itself to the adjacent B-tubule. (ii) The B-tubule imposes a stress on the attached arm to change the angle between the axis of the arm and the A-tubule, and the B-tubule slides past the A-tubule in the direction of the top of the axoneme. (iii) With the binding of another ATP to the active site of the dynein ATPase, the dynein arm detaches itself from the B-tubule and tilts towards the base again. (iv) A more effective coupling between ATP hydrolysis and the cyclic formation of the cross-bridge is achieved through the activation of dynein ATPase activity by (B-)microtubule proteins, that is, the acceleration of the rate of decomposition of enzyme-phosphate complex.

Naitoh and Kaneko (38,56) showed that the direction of the power stroke of Paramecium cilia is controlled by Ca^{2+} around the ciliary systems, and Naitoh (65) proposed that the ciliary system of the Paramecium has at least two kinds of motile components; one is concerned with the cyclic bending of the cilia and the other with regulating the orientation of the effective power stroke of beating cilia. He (66) also reported that the relative effects of various NTP on the reorientation response were ATP>UTP>ITP>GTP>CTP. I found that 2'-dATP and 3'-dATP induced the reorientation of cilia of Tetrahymena, but all the other ATP analogs tested did not. In

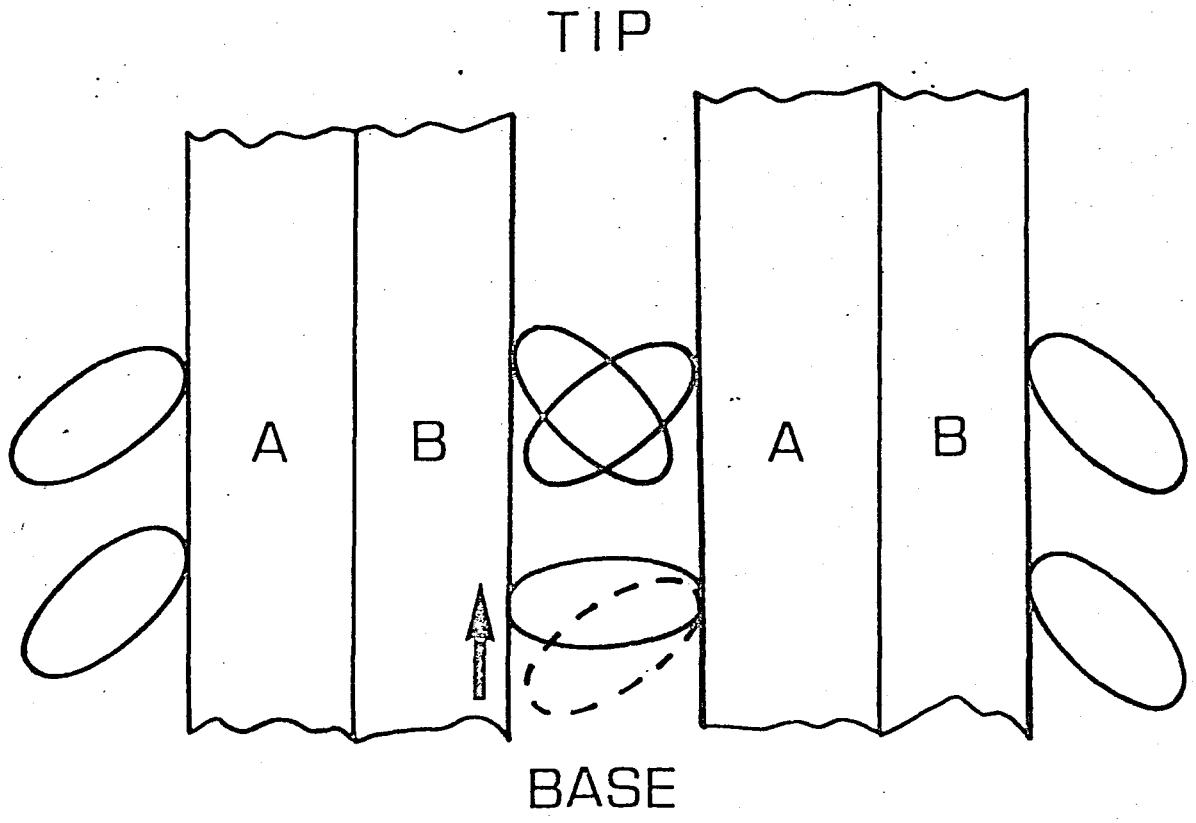

Fig. 20. The diagram explains the hypothesis that the force responsible for sliding between doublets originates from the formation of the cross-bridge itself. A: A-tubule. B: B-tubule. For further explanation, see the text.

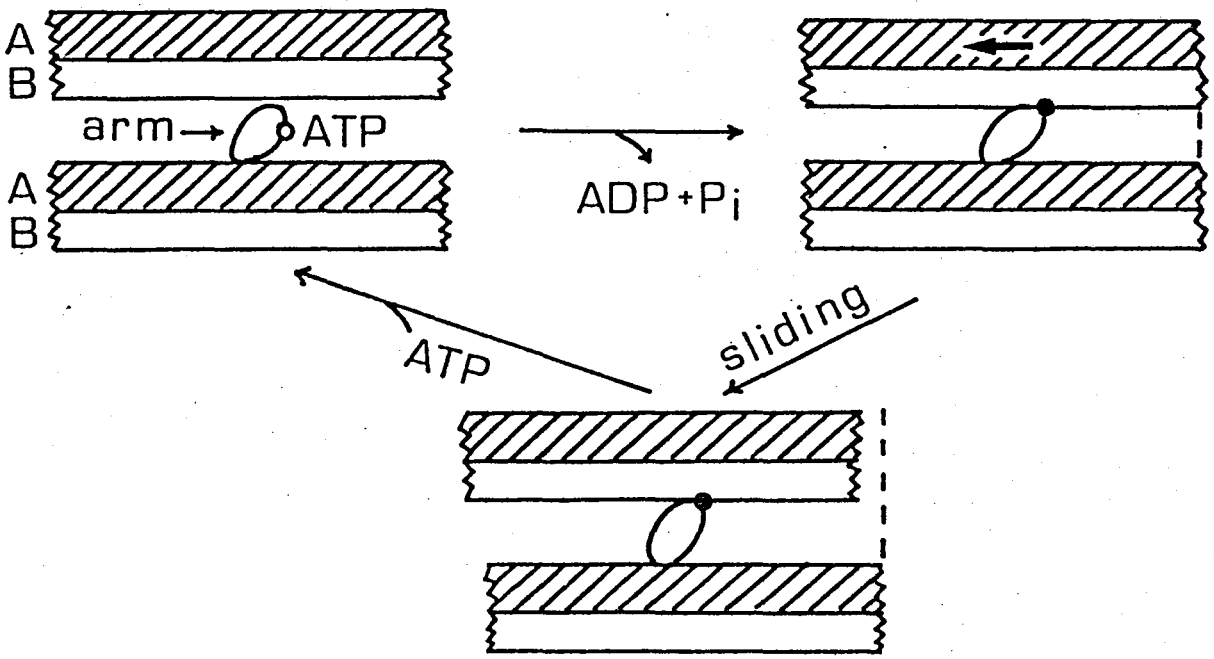

Fig. 22. A molecular model for the active sliding between doublet microtubules. A: A-tubule. B: B-tubule. ○ : ATP-binding site on the arm. ⊙ : ATP-sensitive binding site of the arm for the adjacent B-tubule. For further explanation, see the text.

this respect, this motile system resembles to dynein-tubulin system rather than myosin-actin system.

REFERENCES

1. Sleigh, M. A.(1974) "Cilia and Flagella" Academic Press, New York
2. Mohri, H. (1976) Biochim. Biophys. Acta. 456, 85-127
3. Engelhardt, V. A. (1946) Advan. Enzymol. 6, 147-191
4. Engelhardt, V. A. & Burnasheva, S.A. (1957) Biokhimiya 22, 554
5. Hoffmann-Berling, H. (1955) Biochim. Biophys. Acta 16, 146-154
6. Gibbons, I.R. (1963) Proc. Natl. Acad. Sci. U. S. 50, 1002-1010
7. Gibbons, I. R. (1965) Arch. Biol. (Liege) 76,317-352
8. Ogawa, K., Mohri, T., & Mohri, H. (1977) Proc. Natl. Acad. Sci. U. S. 74, 5006-5010
9. Gibbons, I. R. (1966) J. Biol. Chem. 5590-5596
10. Mohri, H., Hasegawa, S., Yamamoto, M., & Murakami, S. (1969) Sci. Pap. Coll. Gen. Educ. Univ. Tokyo 19, 195-217
11. Mabuchi, I., Shimizu, T., & Mabuchi, Y. (1976) Arch. Biochem. Biophys. 176, 564-576
12. Kimura, I. (1977) J. Biochem. 81, 715-720
13. Burns, R. G. & Pollard, T. D. (1974) FEBS Lett. 40, 274-280
14. Gaskin, F.,Kramer, S. B.,Cantor, C. R., Adelstein, R., & Shelanski, M. L. (1974) EEBS Lett. 40, 281-286
15. Ogawa, K. & Gibbons, I. R. (1976) J. Biol. Chem. 251, 5793-5801
16. Warner, F. D., Mitchell, D. R., & Perkins, C. R. (1977) J. Mol. Biol. 114, 367-384

17. Gibbons, I. R., Cosson, M.P., Evans, J. A., Gibbons, B. H., Houck, B., Martinson, K. H., Sale, W. S., & Tang, W. Y.(1978) Proc. Natl. Acad. Sci. U.S. 75, 2220-2224

18. Gibbons, B. H. & Gibbons, I. R. (1972) J. Cell Biol. 54, 75-97

19. Gibbons, I. R. (1965) J. Cell Biol. 25, 400-402

20. Gibbons, B. H. & Gibbons, I. R. (1973) J. Cell Sci. 13, 337-357

21. Gibbons, B. H. & Gibbons, I. R. (1976) Biochem. Biophys. Res. Commun. 73, 1-6

22. Okuno, M., Ogawa, K., Mohri, H. (1976) Biochem. Biophys. Res. Commun. 68, 901-906

23. Gibbons, B. H., Ogawa, K., & Gibbons, I. R. (1976) J. Cell Biol. 71, 823-831

24. Satir, P. (1968) J. Cell Biol. 39, 77-94

25. Summers, K. E. & Gibbons, I. R. (1971) Proc. Natl. Acad. Sci. U.S. 68, 3092-3096

26. Sale, W. S. & Satir, P. (1977) Proc. Natl. Acad. Sci. U.S. 74, 2045-2049

27. Brokaw, C. J. (1975) in "Molecules and Cell Movement" (Inoue S. & Stephens, R. E.,eds.) pp. 165-179, Raven Press, New York

28. Huxley, A. F. (1974) J. Physiol. 243, 1-43

29. Gibbons, B. H. & Gibbons, I. R. (1974) J. Cell Biol. 63, 970-985

30. Gibbons, I. R. (1975) in "Molecules and Cell Movement" (Inoue, S. & Stephens, R. E.,eds.) pp. 207-232, Raven Press, New York

31. Warner, F. D. & Mitchell, D.R. (1978) J. Cell Biol. 76, 261-

277

32. Gibbons, I. R. & Rowe, A. J. (1965) Science 149, 424-426
33. Inoue, A., Takenaka, H., Arata, T., & Tonomura, Y. (1979) Adv. Biophys. in press
34. Tonomura, Y. (1972) "Muscle Proteins, Muscle Contraction and Cation Transport, Univ. Tokyo Press, Tokyo & Univ. Park Press, Baltimore, MD
35. Onishi, H., Ohtsuka, E., Ikehara, M., & Tonomura, Y. (1973) J. Biochem. 74, 435-450
36. Takenaka, H., Ikehara, M., & Tonomura, Y. (1978) Proc. Natl. Acad. Sci. U.S. 75, 4229-4233
37. Mowery, P. C. (1973) Arch. Biochem. Biophys. 159, 374-377
38. Naitoh, Y. & Kaneko, H. (1973) J. Exp. Biol. 58, 657-676
39. Tiez, A. & Ochoa, S. (1958) Arch. Biochem. Biophys. 78, 477-494
40. Glynn, I. M. & Chappell, J. B. (1964) Biochem. J. 90, 147-149
41. Weber, K. & Osborn, M. (1964) J. Biol. Chem. 244, 4406-4412
42. Hayashi, Y. (1972) J. Biochem. 72, 83-100
43. Kanazawa, T. & Tonomura, Y. (1965) J. Biochem. 57, 604-615
44. Reynard, A. M., Hass, L. F., Jacobsen, D. D., & Boyer, P. D. (1961) J. Biol Chem. 236, 2277
45. Sekiya, K., Takeuchi, K., & Tonomura, Y. (1967) J. Biochem. 61, 567-579
46. Lowry, O. H., Rosebrough, N. J., Farr, A. L. & Randall, R. J. (1951) J. Biol. Chem. 193, 265-275
47. Bensadoun, A. & Weinstein, D. (1976) Anal. Biochem. 70, 241-250

48. Amos, L. A., Linck, R. W., & Klug, A. (1976) in "Cell Motility" (Goldman, R. D., Pollard, T. D., & Rosenbaum, J. L., eds.) pp. 847-867, Cold Spring Harbor Laboratory, Cold Spring Harbor, New York

49. Summers, K. E. & Gibbons, I. R. (1973) J. Cell Biol. 58, 618-629

50. Witman, G. B., Fay, R., & Plummer, J. (1976) in "Cell Motility" (Goldman, R. D., Pollard, T. D., & Rosenbaum, J. L.,eds,) pp. 969-986, Cold Spring Harbor Laboratory, Cold Spring Harbor, New York

51. Gibbons, I. R. (1965) J. Cell Biol. 26, 707-712

52. Warner, F. D. (1974) in "Cilia and Flagella" (Sleigh, M. A. ed.) pp. 11-37, Academic Press, New York

53. Sale, W. S. & Satir, P. (1976) J. Cell Biol. 71, 589-605

54. Gibbons, I. R., Fronk, E., Gibbons, B. H., & Ogawa, K. (1976) in "Cell Motility" (Goldman, R. D., Pollard, T. D., & Rosenbaum J. L., eds.) pp. 915-932, Cold Spring Harbor Laboratory, Cold Spring Harbor, New York

55. Morita, T., Fukui, K., & Asai, H. (1978) Reactivation of Triton-treated Paramecium: Effects of ATP Analogs on Ciliary Movement and Ciliary Reversal (Abst.) presented in Sixth International Biophysics Congress p. 165

56. Naitoh, Y. & Kaneko, H. (1972) Science 176, 523-524

57. Shimizu, T. (1975) J.Biochem. 78, 41-49

58. Ogawa, K. (1973) Biochim. Biophys. Acta 293, 514-525

59. Warner, F. D. (1978) J. Cell Biol. 77, R19-R26

60. Hoshino, M. (1977) Biochim. Biophys. Acta 492, 70-82

61. Nakamura, K. & Masuyama, E. (1977) Biochim. Biophys. Acta 481, 660-666

62. Otokawa, M. (1972) Biochim. Biophys. Acta 275, 464-466

63. Blum, J. J. & Hayes, A. (1974) Biochemistry 13, 4290-4298

64. Hoshino, M. (1976) Biochim. Biophys. Acta 462, 49-62

65. Naitoh, Y. (1966) Science 154, 660-662

66. Naitoh, Y. (1969) J. Gen. Physiol. 53, 517-529

ACKNOWLEDGMENT

The author would like to express my great appreciation to Professor Yuji Tonomura of Osaka University for his kind guidance, many valuable suggestions, and continuous encouragement during the course of this work. The author is also greatly indebted to Dr. Kiyoko Kuroda of Osaka University for providing a stock culture of Tetrahymena and for her kind advice on light microscopy, to Drs. Kikuko Takeuchi and Reiko Nagai of Osaka University for their advice on electron microscopy, and to Dr. Hitoshi Takenaka for providing me various ATP analogs. The author is pleased to acknowledge the valuable discussion of all the members of Tonomura-Laboratory of Osaka University.

SUMMARY

(I) The binding properties of dynein arms to the A- and B-tubules of outer doublets of cilia.

1. When 30s dynein purified from Tetrahymena cilia was added to doublets deficient in dynein arms, it bound to both A- and B-tubules almost equally and formed arms along the edges. The overall length of arms bound to the A-tubule was 22 ± 3 nm, and that of arms bound to the B-tubule was 24 ± 3 nm. Each arm bound to the A- and B-tubules was pointed toward the base at angles of 55° ± 7° and 48° ± 7°, respectively. In the presence of sufficient amounts of dynein, the arms along the A- and B-tubules were located at intervals of 22.8 ± 1.5 nm and 22.5 ± 1.7 nm, respectively.

2. On adding ATP, only the arms bound to the B-tubule were dissociated from the doublet decorated with arms on both sides. The dissociated arms rebound themselves to the B-tubule after hydrolysis of the ATP. When several doublets decorated with arms along both A- and B-tubules were arrayed side by side, the interdoublet spacing increased from 14 ± 2 nm to 17 ± 2 nm on addition of ATP.

3. The turbidity of a suspension of trypsin [EC 3.4.21.4]-treated axonemes decreased rapidly on addition of ATP, then recovered partially. Observations by dark-field microscopy and electron microscopy showed that the doublets which had slid out from the axonemes on ATP addition formed large aggregates after hydrolysis of the ATP. The dynein arms were also solubilized from the axonemes upon addition of ATP, and rebound

themselves to the B-tubule after hydrolysis of the added ATP.

4. The double reciprocal plot for the ATPase [EC 3.6.1.3] activity of the trypsin-treated axoneme against ATP concentration was composed of two straight lines, from which the K_m values were estimated to be 1.0 and 12.7 μM. The dependence of the decrease in turbidity of the axonemal suspension on ATP concentration indicated that the binding of ATP to sites with an apparent dissociation constant of 1 μM induced dissociation of the arms from the B-tubule.

(II) Kinetic properties of dynein ATPase.

1. Dynein was extracted with 0.5 M KCl from Tetrahymena axonemes. SDS-gel electrophoresis of the extract indicated that about 50% of the extracted protein had a molecular weight of about 3.5 x 10^5 daltons, and that 90% of the proteins with this weight had been extracted.

2. The ATPase reaction of the KCl-extracted dynein fraction was enhanced by 60-80% by addition of the outer doublet fraction. It showed an initial burst of P_i liberation of about 1 mol per mol of 3.5 x 10^5 dalton proteins.

3. I examined the interaction of the dynein-tubulin system from Tetrahymena cilia with ten ATP analogs [2'-dATP, 3'-dATP, ε ATP, FTP, 8-$NH(CH_3)$-ATP, 8,3'-S-cyclo-ATP, 8-Br-ATP, 8-SCH_3-ATP, 8-OCH_3-ATP, and AMPPNP]. Among them, 2'-dATP and 3'-dATP were good substrates for dynein ATPase, as they induced the dissociation of dynein arms from the B-tubule of outer doublets, the sliding movement between outer doublets, and the bending movement of axonemes, the other analogs did not induce the dissociation

or the sliding movement.

4. Among the ATP analogs tested, only 2'-dATP and 3'-dATP induced the reorientation of cilia on the Triton model of Tetrahymena; the reorientation rates were smaller than that induced by ATP.